Natural Hazards (2026) 122:224
https://doi.org/10.1007/s11069-025-07961-2

ORIGINAL PAPER

# Multi-Index evaluation of meteorological drought across Türkiye: a temporal and seasonal perspective

**Bülent Selek**[1] · **Murat Pinarlik**[2] · **Ismail Faki**[3] · **Zeliha Selek**[2]

Received: 19 July 2025 / Accepted: 27 December 2025
© The Author(s) 2026

**Abstract**
Türkiye, situated in the Mediterranean Basin, is highly susceptible to drought due to its predominantly semi-arid climate. This study aims to evaluate the temporal and seasonal dynamics of drought across Türkiye by employing three distinct drought indices: the Standardized Precipitation Index (SPI), the Standardized Precipitation Evapotranspiration Index (SPEI), and the Percent of Normal Index (PNI). Long-term spanning the period 1972–2023, monthly areal average precipitation data derived through Kriging interpolation and monthly average temperature data from 255 meteorological stations were used. Drought assessments were conducted on both monthly and seasonal scales, with SPI and SPEI calculated at 3-, 6-, 9-, 12-, and 24-month timescales to capture meteorological, agricultural, and hydrological drought characteristics. The results revealed that the most severe drought occurred during 2007–2009 with nationwide SPI values dropping below −2.0. Severe droughts (SPI < −1.5) were observed in approximately 18% of the study period, with summer droughts being 30–35% more frequent than winter droughts. During 2020–2023, more than 70% of stations simultaneously experienced drought conditions, highlighting the increasing influence of temperature-driven evapotranspiration. Notably, SPEI values were consistently lower than SPI during summer and autumn, reflecting the intensifying role of rising temperatures and Potential Evapotranspiration (PET), while PNI corroborated these findings and emphasized Türkiye's heightened drought sensitivity during the summer season. This study demonstrates the added value of temperature-based indices in drought monitoring and provides essential insights for, drought early warning systems, and water resource management in drought-prone regions. The Mann–Kendall analysis indicates an overall increase in drought severity after 2000, marked by temperature-driven summer drying and a slight winter wetting tendency.

**Keywords** SPI · SPEI · PNI · Drought · Türkiye · Mann-Kendal

Extended author information available on the last page of the article

Published online: 25 February 2026

## 1 Introduction

Drought is a natural disaster that significantly affects water resources and, consequently, agriculture and socio-economic activities (Ojha et al. 2021; Politi et al. 2022). With the intensifying impacts of global climate change, both the frequency and severity of droughts have shown a concerning upward trend (Zhao and Wang 2020). Therefore, analysing the characteristics of drought has become a necessity for developing drought-resilient water management policies and strategies (Liu et al. 2016; Zhao et al. 2021a, b).

Located at the intersection of different climate zones, Türkiye experiences a wide variety of precipitation and temperature regimes. This climatic variability leads to drought events of varying intensity and duration across the country's 26 hydrological basins (Yiğit and Keten 2024). Therefore, accurately assessing drought conditions in Türkiye is of great importance for developing effective adaptation strategies against this hazard. In one study, Bagnouls-Gaussen drought indices were calculated using precipitation and temperature data from the provincial centres of Türkiye for the period 2000–2016. The results classified 24 provinces as "very arid," 37 as "arid," 12 as "semi-humid," and 8 as "humid" (Cebeci et al. 2019). According to data from the Turkish State Meteorological Service (TSMS), the 2020/2021 hydrological-agricultural year began with meteorological drought conditions, as winter precipitation across much of the country was 20% to 40% below normal levels. In some regions, this situation escalated to hydrological drought levels (Yıldız and Özgüler 2021). In a nationwide study conducted by Selek et al. (2018) using the Thornthwaite method, a comparison of two 30-year periods (1950–1980 and 1981–2010) revealed an increase in semi-arid and dry-humid areas, and a decrease in semi-humid, slightly humid, and humid zones.

Temporal drought analysis is a critical approach aimed at identifying drought trends by evaluating long-term precipitation and temperature data. In this context, the most commonly used methods include the Standardized Precipitation Index (SPI) (McKee et al. 1993), the Standardized Precipitation Evapotranspiration Index (SPEI) (Vicente-Serrano et al. 2010), and the Palmer Drought Severity Index (PDSI) (Palmer 1965). Stagge et al. (2015) systematically evaluated the suitability of alternative probability distributions for SPI and SPEI standardization across Europe, improving the statistical robustness of index estimation. Lee et al. (2024) quantified the sensitivity of SPEI to different PET estimation methods, highlighting how the choice of climatic inputs can influence temporal and spatial drought patterns. Beyond the parametric formulation, Farahmand and AghaKouchak (2015) proposed a non-parametric Standardized Drought Analysis Framework (SDAT), reducing distributional assumptions and improving robustness under data-limited conditions. More recently, the development of a global daily multi-scale SPEI dataset has further expanded the temporal resolution and monitoring capability of drought analyses (Liu et al. 2024). SPI assesses precipitation data over various time scales (e.g., 1, 3, 6, 12, and 24 months) based on a standard normal distribution (Tirivarombo et al. 2018). A month scale typically reflects meteorological drought, 3–6 months represent agricultural drought, and 12 months is indicative of hydrological drought (Vicente-Serrano et al. 2010; Homdee et al. 2016). However, since SPI relies solely on precipitation data, it does not account for the effects of temperature variations and evaporation processes on drought (Gumus 2023). SPEI was also developed to evaluate the impact of temperature fluctuations on drought (Meseguer-Ruiz 2024). In addition to using procedures similar to SPI, it incorporates the calculation of PET using established methods such as Thornthwaite or Penman (Thornthwaite 1948; Ortiz-Gómez et

al., 2022). The Palmer Drought Severity Index (PDSI), on the other hand, considers changes in soil moisture and is widely used in agricultural and hydrological drought assessments (Wang et al. 2015; Zhao et al. 2017). Over the past decade, numerous comparative studies of SPI and SPEI have been conducted at both national and basin scales (Wang et al. 2019; Pei et al. 2020; Danandeh Mehr and Vaheddoost 2020; Zarei et al. 2021; Nwayor and Robeson 2024). In recent years, alongside conventional indices, machine learning (ML)-based models have been increasingly applied for drought prediction and time series analysis (Mokhtar et al. 2021). These include Artificial Neural Networks (ANNs) (Moreno et al. 2011; Kumar et al. 2015), Support Vector Machines (SVMs) (Quej et al. 2017; Fan et al. 2018), tree-based models (e.g., Random Forest, XGBoost) (Hassan et al. 2017; Papadopoulos et al. 2018; Zhang et al. 2019), and Long Short-Term Memory networks (LSTM) (Dikshit et al. 2021; Tuğrul et al. 2025).

In recent years, some studies in Türkiye have employed stochastic and graphical trend analysis techniques to evaluate the impacts of climate change on regional hydro-meteorological conditions. Ceyhunlu and Ceribasi (2024a) applied Seasonal Autoregressive Integrated Moving Average (SARIMA)-based stochastic time-series models to forecast precipitation and temperature patterns across Türkiye up to 2050, integrating the results with Standardized Precipitation Evapotranspiration Index (SPEI)-based drought projections to produce nationwide drought maps. In another study (Ceyhunlu and Ceribasi 2024b) utilized the Innovative Trend Pivot Analysis Method (ITPAM) to assess 30-year precipitation and air temperature data for all provinces, revealing widespread warming trends and demonstrating the method's non-parametric and risk-oriented capability in detecting climate variability. Similarly, Simsek et al. (2024) employed the Crossing Empirical Trend Analysis (CETA) to examine long-term meteorological drought conditions in the Aras and Çoruh Basins, indicating an overall increase in drought tendencies and highlighting CETA's strength in capturing nonlinear and extreme-value-driven trends.

Recent advances in remote sensing products have substantially contributed to large-scale drought monitoring by providing spatially continuous and temporally consistent information beyond conventional station-based observations. Satellite-derived vegetation indices from sensors such as MODIS have been widely employed to assess vegetation stress and surface conditions, enabling the detection of drought impacts across broad regions and diverse climatic settings (Zhao et al. 2021a, b; Ha et al. 2023). In parallel, GRACE satellite observations allow the monitoring of terrestrial water storage anomalies, offering an integrated representation of surface and subsurface water components and thereby supporting the assessment of large-scale hydrological drought dynamics (Rawat et al. 2022; Cui et al. 2024). In addition, satellite-based precipitation products such as the Climate Hazards Group InfraRed Precipitation with Stations (CHIRPS) have been extensively used in meteorological drought studies due to their high spatial resolution, long-term coverage, and ability to complement sparse gauge networks (Ghozat et al. 2022; Aksu et al. 2022). Together, these remote sensing approaches have become an important component of national- and continental-scale drought assessments. Nevertheless, their relatively shorter record lengths, verification requirements through ground-based observations and indirect representation of climatic processes highlight the continued importance of long-term in-situ observations for robust historical drought characterization and trend analysis.

While the analytical framework of this study builds on widely applied drought indices (SPI, SPEI, and PNI), its primary novelty lies in the unprecedented spatial and temporal

comprehensiveness of the dataset covering 255 meteorological stations across Türkiye over a 52-year period. The use of areal precipitation data generated through Kriging interpolation (Selek and Aksu 2020) ensures a realistic spatial representation of rainfall distribution and strengthens the reliability of drought assessments across diverse climatic regions. Moreover, by employing both the Standardized Precipitation Index (SPI) and the Standardized Precipitation Evapotranspiration Index (SPEI), the study provides a more integrated assessment that considers not only precipitation variability but also temperature-driven evapotranspiration effects. Unlike spatial pattern analyses, the focus here is on the temporal dynamics of drought, offering valuable insights for monitoring and management of drought. The scarcity of long-term, nationwide drought studies specific to Türkiye further underscores the relevance of this research.

In addition to its large-scale scope, this study applies three complementary drought indices (SPI, SPEI, and PNI) across multiple temporal scales (1-, 3-, 6-, 9-, and 12-month) to enhance comparative evaluation. Spatial aggregation based on Ordinary Kriging with an exponential model provides consistent areal precipitation fields, ensuring higher spatial reliability in drought characterization. Through this multi-index, multi-scale, and interpolation-based framework, the study offers a comprehensive foundation for assessing both precipitation- and temperature-driven drought dynamics across Türkiye. Furthermore, the approach provides transferable methodological insights for drought monitoring and climate adaptation in other semi-arid and topographically heterogeneous regions.

Methodologically, in the first stage, a nationwide drought analysis was conducted using the SPI method based on areal precipitation data. In the second stage, monthly mean temperature data were incorporated into the SPEI method to assess the combined influence of precipitation and evapotranspiration. This dual analysis enabled a clearer evaluation of the separate and joint impacts of temperature and precipitation on drought severity and duration across different temporal scales.

In addition to multi-index drought characterization, a Mann–Kendall (MK) trend analysis was applied to detect the long-term direction and statistical significance of drought tendencies. This complementary approach provides quantitative insight into whether recent decades have experienced a transition toward persistent temperature-driven drought regimes across Türkiye.

## 2 Materials and methods

### 2.1 Study area and data set

Türkiye is located between 36° and 42° north latitudes and 26° and 45° east longitudes, and is generally characterized by semi-arid climatic conditions. However, the country's geographic and topographic diversity leads to significant variations in the distribution of precipitation and temperature. In a study conducted by the Turkish State Meteorological Service, the average areal precipitation across Türkiye was calculated using data from 255 meteorological stations covering the period from 1981 to 2010 and extended to 1972–2023 later. The areal precipitation values were derived based on results obtained using the Ordinary Kriging Exponential technique. The precipitation distribution generated through this

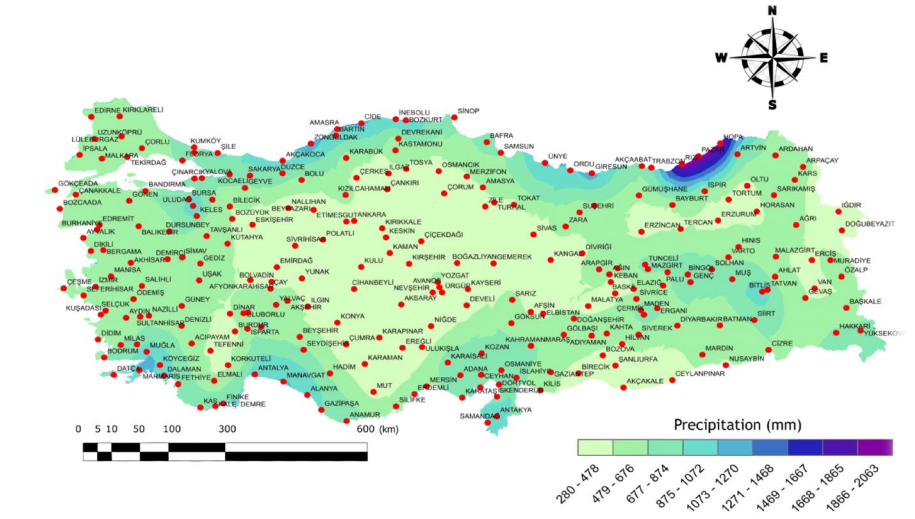



**Fig. 1** Distribution of meteorological stations and areal precipitation in Türkiye (Turkish State Meteorological Service 2016)

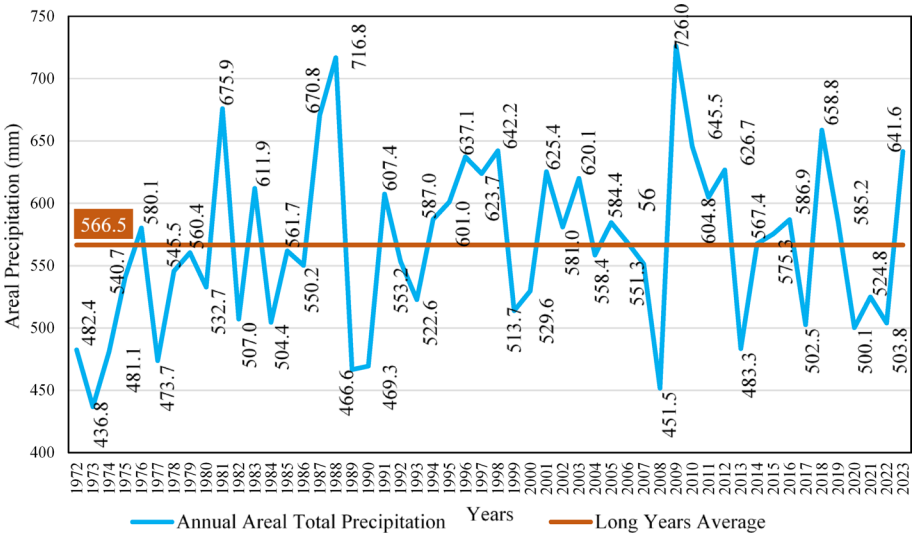



**Fig. 2** Annual areal total precipitation of Türkiye (1972–2023)

method is illustrated in Fig. 1 (Ulupinar et al. 2015). The areal precipitation data used in the present study were obtained from the aforementioned official dataset.

The annual areal average precipitation values for the period 1972–2023 considered in this study are presented in Fig. 2. The percentage changes in precipitation between consecutive years are shown in Fig. 3, revealing interannual variability. The long-term precipita-

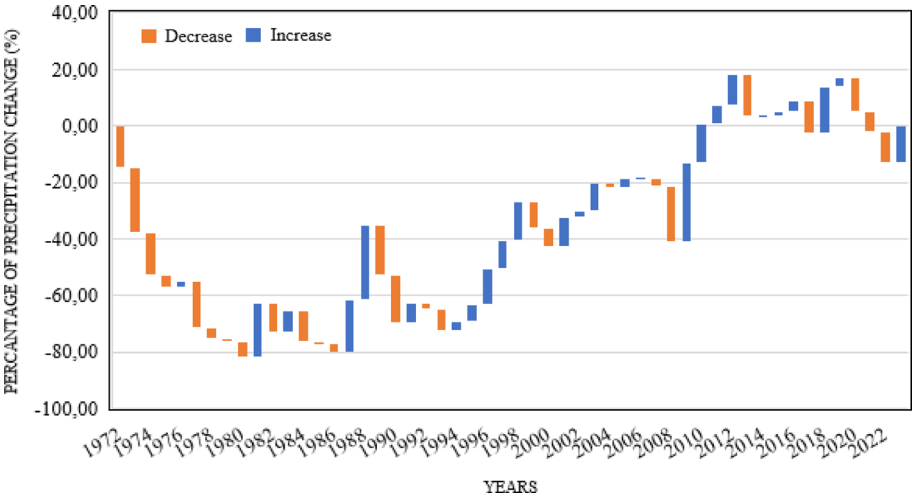



**Fig. 3** Annual changes of precipitation (%)

tion and temperature records for this period exhibit noticeable fluctuations across Türkiye. Annual areal average precipitation ranged between 436.8 mm (in 1972) and 726.0 mm (in 2010), with a long-term mean of 566.5 mm. The standard deviation of the precipitation series was 73 mm, corresponding to a coefficient of variation (CV) of 12.9%, indicating a moderate level of interannual variability without a distinct monotonic trend.

During the same period, the mean annual temperature was 13.6 °C, with the lowest value of 11.7 °C (in 1992) and the highest of 15.5 °C (in 2011). The standard deviation of the temperature series was approximately 0.9 °C, yielding a CV of 6.6%. The analysis results indicate a statistically significant warming trend across Türkiye, corresponding to an increase of approximately 0.30 °C per decade. The temporal distribution of annual average temperatures is illustrated in Fig. 4, while Fig. 5 visualizes the percentage change in temperature between successive years, highlighting year-to-year fluctuations. Air temperature records were obtained from the same network of meteorological stations and aggregated to derive national-scale average temperature series consistent with the precipitation dataset.

The dataset used in this study consists of monthly precipitation and air temperature records obtained from the Turkish State Meteorological Service of Türkiye, which serves as an official authority for national hydrometeorological data archiving. The dataset covers the period 1972–2023 and includes observations from 255 meteorological stations distributed across Türkiye. Monthly values were derived from quality-controlled station records and used consistently for all drought index calculations.

Prior to analysis, the data were screened for completeness and consistency. Stations with substantial data gaps were excluded to ensure temporal continuity, and the remaining records were aggregated to derive nationwide areal precipitation series using the Ordinary Kriging method with an exponential semi variogram model. This approach provides spatially continuous representations of precipitation while maintaining consistency across the long-term national dataset. No additional homogenization procedures were applied beyond basic completeness screening, and the analysis relies on the consistency of the official archived records.

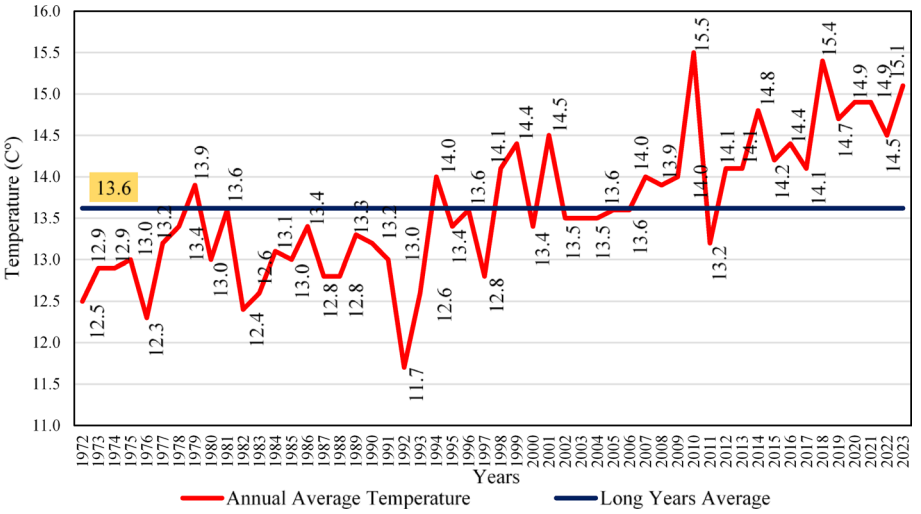



**Fig. 4** Annual average temperature (C°) graph of Türkiye (1972–2023)

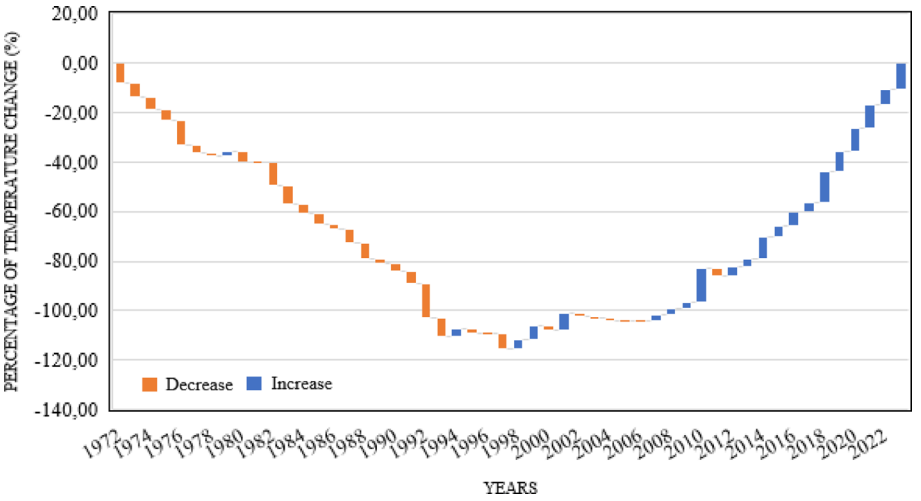



**Fig. 5** Changes of temperature (%)

## 2.2 Methodology

The overall structure and methodological framework of the study are presented in Fig. 6. The flowchart summarizes the main stages, including data acquisition (precipitation and temperature), drought index computations (SPI, SPEI, and PNI), temporal and comparative analyses, trend analyses and the final interpretation of drought variability across Türkiye.

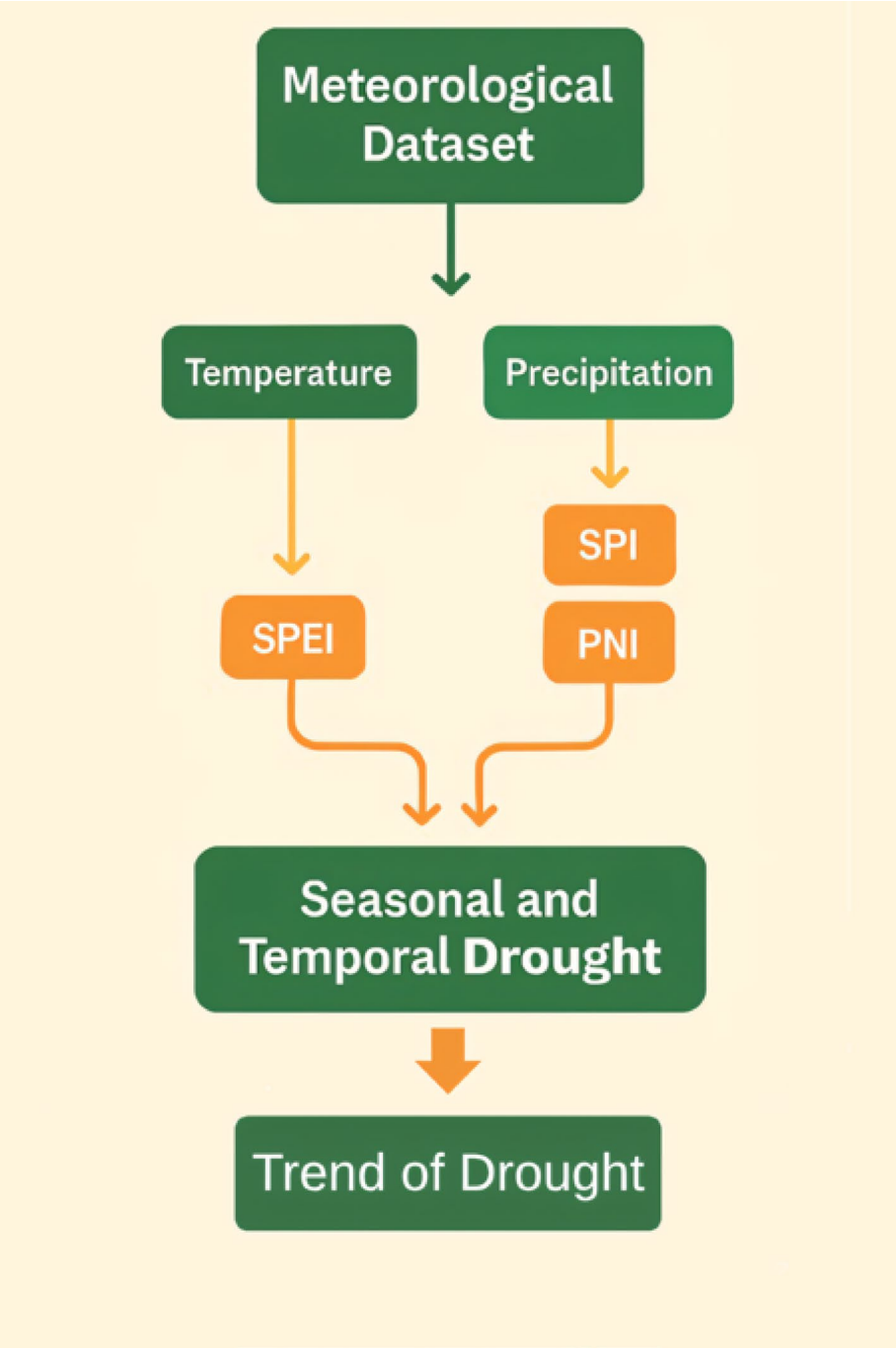



**Fig. 6** Methodological framework of the study

### 2.2.1 Standardized precipitation index (SPI)

The Standardized Precipitation Index (SPI) was developed by McKee et al. (1993) to better understand reductions in precipitation and to evaluate their effects on groundwater, reservoir storage, soil moisture, snowpack, and streamflow. SPI involves fitting a suitable probability density function to precipitation data recorded at meteorological stations.

Thom (1958) demonstrated that the gamma distribution provides an appropriate and widely applicable fit for climatic precipitation series, which led to its adoption in the original formulation of the SPI (see Eqs. 1 and 2).

$$g\left(x\right)=\frac{1}{\beta^{a}\Gamma\left(a\right)}x^{a-1}\mathrm{e}^{-x/\beta} \tag{1}$$

The parameters in Eq. 1 are defined as follows: $\alpha>0$ is the shape parameter, $\beta>0$ is the scale parameter, and $x>0$ represents the amount of precipitation. Equation 2 defines the gamma function.

$$\Gamma\ \left(a\right)=\int_{0}^{\infty}y^{a-1}e^{-y}dy \tag{2}$$

According to Thom (1966), the most appropriate estimation equations for the shape parameter (α) and the scale parameter (β), based on the method of maximum likelihood estimation, are given in Eqs. 3 and 4, respectively.

$$\widehat{a}=\frac{1}{4A}\left(1+\sqrt{1+\frac{4A}{3}}\right) \tag{3}$$

$$\widehat{\beta}\ =\frac{\bar{x}}{\widehat{a}} \tag{4}$$

For a precipitation dataset consisting of n values, the parameter A is calculated using Eq. 5.

$$A=\ln\left(\bar{x}\right)-\frac{\sum\ln\left(x\right)}{n} \tag{5}$$

Using the estimated $\widehat{a},\widehat{\beta}$, the cumulative gamma probability density function is obtained as given in Eq. 6.

$$G\left(x\right)=\int_{0}^{x}\mathrm{g}\left(\mathrm{x}\right)dx=\frac{1}{\hat{\beta}^{\hat{a}}\Gamma\left(\hat{a}\right)}\int_{0}^{x}x^{\hat{a}-1}\mathrm{e}^{-x/\hat{\beta}}\,dx \tag{6}$$

By substituting $t=x/\beta$, Eq. 7 is derived as follows.

$$G(x) = \frac{1}{\Gamma(\widehat{a})} \int_0^x t^{\widehat{a}} e^{-1} dt \tag{7}$$

The gamma function is undefined at x = 0, while precipitation data often include zero values corresponding to dry days.

Cumulative Probability Distribution Function:

$$H(x) = q + (1 - q)G(x) \tag{8}$$

In Eq. 8, q represents the percentage of zero-precipitation days. In Eq. 9, m denotes the number of dry days in the precipitation time series.

$$q = m/n \tag{9}$$

The cumulative probability distribution function H(x), transforms precipitation values into standard normal random variables with a mean of 0 and a variance of 1.

The equations provided by Abramowitz and Stegun (1965) are used to convert the cumulative probability distribution function H(x) into standardized Z-SPI values.

When the value of H(x) falls within the range $0 < H(x) \leq 0.5$ the corresponding Z values are calculated using Eq. 10.

$$Z = SPI = -\left(t - \frac{c_0 + c_1 t + c_2 t^2}{1 + d_1 t + d_2 t^2 + d_3 t^3}\right) \quad 0 < \mathrm{H(x)} = 0.5 \tag{10}$$

When the value of H(x) falls within the range $0.5 < H(x) < 1.0$ the corresponding Z values are calculated using Eq. 11.

$$Z = SPI = +\left(t - \frac{c_0 + c_1 t + c_2 t^2}{1 + d_1 t + d_2 t^2 + d_3 t^3}\right) \quad 0.5 < \mathrm{H(x)} < 1.0 \tag{11}$$

In Eqs. 10 and 11, the *t* values are calculated accordingly.

$$t = \sqrt{\ln \frac{1}{(H(x))^2}} \quad 0 < \mathrm{H(x)} \leq 0.5 \tag{12}$$

$$t = \sqrt{\ln \frac{1}{(1 - (H(x))^2}} \quad 0.5 < \mathrm{H(x)} < 1.0 \tag{13}$$

The constant values used in Eqs. 10 and 11 are given below.

$c_0 = 2.515517$, $c_1 = 0.802853$, $c_2 = 0.010328$, $d_1 = 1.432788$, $d_2 = 0.189269$, $d_3 = 0.001308$ (Sırdaş 2002).

Z-SPI values can take both positive and negative values. The drought values and classification categories for SPI and SPEI are presented in Table 1.

**Table 1** Drought categories corresponding to SPI and SPEI values (McKee et al. 1993)

| SPI values | Drought categories |
|---|---|
| >2.00 | Extremely wet |
| 1.50 to 1.99 | Very wet |
| 1.00 to 1.49 | Moderately wet |
| 0.99 to − 0.99 | Near normal |
| − 1.00 to − 1.49 | Moderately dry |
| − 1.50 to − 1.99 | Severely dry |
| ≤ − 2.00 | Extremely dry |

The Standardized Precipitation Index (SPI) was calculated in this study using the two-parameter Gamma distribution, which has been traditionally adopted in the original SPI formulation (Thom 1958, 1966). The Gamma distribution was employed to ensure methodological consistency with the classical SPI framework and is not assumed to be universally optimal for all climatic conditions.

While the Gamma distribution has been widely used in SPI applications, recent studies have demonstrated that alternative probability distributions, such as Pearson Type III, Generalized Extreme Value (GEV), Weibull, and Log-Logistic, may also be suitable for drought analysis depending on regional climate characteristics and temporal scale (Guttman 1999; Mahmoudi et al. 2019; Pieper et al. 2020; Yılmaz et al. 2023). In this study, the Standardized Precipitation Evapotranspiration Index (SPEI) was computed using the three-parameter log-logistic distribution. The consistency observed between SPI and SPEI across different timescales reflects the applicability of the selected distributions for the large-scale areal precipitation dataset of Türkiye.

### 2.2.2 Standardized precipitation evapotranspiration index (SPEI)

The calculation of SPEI is based on the original SPI computation procedure. While SPI is calculated using monthly (or weekly) precipitation as input data, SPEI uses the monthly (or weekly) difference between precipitation and potential evapotranspiration (PET).

Thornthwaite (1948) represents a simple climatic water balance that is temperature-dependent and used to calculate SPEI at different time scales. Following this method, monthly PET (in mm) is computed as follows.

$$\mathrm{PET} = 16\mathrm{K}\left(\frac{10\mathrm{T}}{\mathrm{I}}\right)^{\mathrm{m}} \tag{14}$$

T: Monthly mean temperature, I: Heat index, m: A coefficient dependent on the value of I. ($\mathrm{m} = 6.75\times10^{-7}\,\mathrm{I}^3 - 7.71\times10^{-5}\,\mathrm{I}^2 + 1.79\times10^{-2}\,\mathrm{I} + 0.492$)

The parameter i, calculated as the sum of 12 monthly index values, is derived from the mean monthly temperature using a specific formula.

$$i = \left(\frac{T}{5}\right)^{1.514} \tag{15}$$

*K* is a correction coefficient calculated as a function of latitude and month.

$$K = \left(\frac{N}{12}\right)\left(\frac{NDM}{30}\right) \tag{16}$$

here *NDM* represents the number of days in the month, and *N* denotes the maximum possible sunshine duration (in hours).

$$N = \left(\frac{24}{\pi}\right)\bar{\omega}_s \tag{17}$$

is the sunset hour angle, and it is calculated using the following formula.

$\bar{\omega}_s = arccos\,(-tan\phi\,.tan\delta\,)$ ($\phi$ is the latitude in radians, and $\delta$ is the solar declination in radians; both are calculated using the following expressions).

$$\delta = 0.4093\text{sen}\left(\frac{2\pi\,J}{365} - 1.405\right) \quad \text{(Here, J is the mean Julian day of the month.)} \tag{18}$$

For the PET value, the difference between precipitation (P) and PET for month i is calculated as follows.

$$D_i = P_i - PET_i \tag{19}$$

The difference $D^k_{i,j}$ for a given month *j* and year *i* depends on the selected time scale *k*. For example, the total difference for a specific month in a given year with a 12-month time scale is calculated as follows:

If j<k then;

$$X^k_{i,j} = \sum{}^{12}_{l=13-k+j} D_{i-1,l} + \sum{}^{j}_{l=1} D_{i,l} \tag{20}$$

If j≥k then;

$$X^k_{i,j} = \sum{}^{j}_{l=j-k+1} D_{i,l} \tag{21}$$

here $D_{i,l}$, represents the difference between precipitation (P) and PET for the first month of year i (mm).

Vicente-Serrano et al. (2010) recommend the use of the log-logistic distribution to standardize the D series for the calculation of SPEI.

$$F(x) = \left[1 + \left(\frac{}{x-\gamma}\right)\right]^{-1} \tag{22}$$

Following the classical approach of Abramowitz and Stegun (1965),

$$SPEI = W - \left(t - \frac{C_0 + C_1 W + C_2 W^2}{1 + d_1 W + d_2 W^2 + d_3 W^3}\right) \tag{23}$$

For $P \leq 0.5$, $W = \sqrt{-2\ln(P)}$ and for $P > 0.5$, $W = \sqrt{-2\ln(1-P)}$ and Constants: $C_0 = 2.515517$, $C_1 = 0.802853$, $C_2 = 0.010328$, $d_1 = 1.432788$, $d_2 = 0.189269$, $d_3 = 0.001308$.

The mean value of SPEI is 0, and its standard deviation is 1. As a standardized variable, SPEI can be compared across both time and space with other SPEI values.

The potential evapotranspiration (PET) was estimated using the Thornthwaite (1948) method, which computes PET based on mean air temperature and latitude-derived day length. Although several approaches exist for PET estimation, including the Penman–Monteith and Hargreaves methods, the required parameters such as solar radiation, relative humidity, and wind speed are not available for all 255 meteorological stations used in this study. Therefore, the Thornthwaite method was selected because it enables a consistent and long-term computation of PET across Türkiye.

Previous studies have shown that, despite its relative simplicity, the Thornthwaite-based PET performs adequately in large-scale drought assessments. In particular, Vicente-Serrano et al. (2010), who developed the Standardized Precipitation Evapotranspiration Index (SPEI), demonstrated that Thornthwaite derived PET values are sufficiently reliable for assessing drought variability over broad spatial domains. Similarly, Mavromatis (2007) reported that both simple and complex PET estimation approaches yield comparable results in long-term drought analyses. Considering these findings, the application of the Thornthwaite method in this study ensures temporal continuity and methodological consistency across all observation stations.

### 2.2.3 Percent of normal index (PNI)

The Percent of Normal Index (PNI) is defined as the ratio of a given precipitation amount to the 30-year arithmetic mean precipitation considered the "normal" for that location. It can be applied over different time scales (daily, weekly, monthly, or annually). An important consideration in the calculation is that when using hydro-meteorological variables recorded over periods shorter than one year, the median should be used instead of the arithmetic mean. As shown in Eq. 24, the PNI is calculated by dividing the *i*-th precipitation value by the long-term mean precipitation (Şen 2009). PNI method drought categories are given in Table 2.

$$N = 100\frac{x_i}{\bar{x}} \tag{24}$$

$x_i$: The *i*-th precipitation value, $\bar{x}$: The long-term mean precipitation value.

The Standardized Precipitation Index (SPI) is widely used for practical meteorological drought assessment because it requires only precipitation data, making it applicable in data-scarce regions. It can be computed at multiple time scales, allowing the identification of

**Table 2** Drought categories corresponding to PNI values (Willeke et al. 1994)

| Period | Normal and Above | Mild Drought | Moderate Drought | Severe Drought |
|---|---|---|---|---|
| 1 | >75 | 65–75 | 55–65 | <55 |
| 3 | >75 | 65–75 | 55–65 | <55 |
| 6 | >80 | 70–80 | 60–70 | <60 |
| 9 | >83.5 | 73.5–83.5 | 63.5–73.5 | <63.5 |
| 12 | >85 | 75–85 | 65–75 | <65 |

short- and long-term droughts and facilitating spatial comparison across different climatic zones. However, its main limitation is that it does not account for evapotranspiration or soil water balance, and thus may underestimate drought severity under warming conditions.

The Standardized Precipitation Evapotranspiration Index (SPEI) differs fundamentally from SPI by incorporating the difference between precipitation and potential evapotranspiration (PET). This feature makes it more sensitive to temperature variations and better suited for evaluating the impacts of climate warming on drought intensity and duration. Nevertheless, its accuracy depends on the PET estimation method, which can introduce additional uncertainty.

In addition to these standardized indices, the Percent of Normal Index (PNI) was also employed as a complementary indicator to provide a simple, percentage-based representation of precipitation anomalies. The inclusion of PNI enables a direct comparison between standardized (SPI and SPEI) and non-standardized approaches, allowing the evaluation of how normalization affects the characterization of drought intensity and frequency. Moreover, PNI serves as a practically interpretable metric that facilitates the communication of drought conditions to non-specialist audiences and decision-makers. Importantly, the Turkish State Meteorological Service (TSMS) officially employs PNI-based results to generate and publish regional drought maps on its national web portal (Turkish State Meteorological Service 2025). Therefore, incorporating PNI into the present study ensures methodological consistency with national drought monitoring practices and enhances the institutional applicability of the results within Türkiye's water resource management framework.

The SPI, SPEI, and PNI series presented in this study were derived from nationwide areal averages rather than single-station data. Precipitation data were spatially interpolated using the Ordinary Kriging (exponential model) method based on 255 meteorological stations to obtain areal precipitation fields, while temperature data were incorporated as monthly mean values directly provided by the Turkish State Meteorological Service (TSMS). Accordingly, the SPI and SPEI time-series graphs (Figs. 6, 7, 8, 9, 10, 11, 12, 13 and 14) represent spatially averaged, temporally continuous drought indices for the entirety of Türkiye. This approach ensures that the results reflect national-scale drought characteristics while minimizing the influence of localized variability.

Together, these three indices complement each other by capturing different dimensions of meteorological drought, ranging from precipitation deficits to temperature-driven mois-

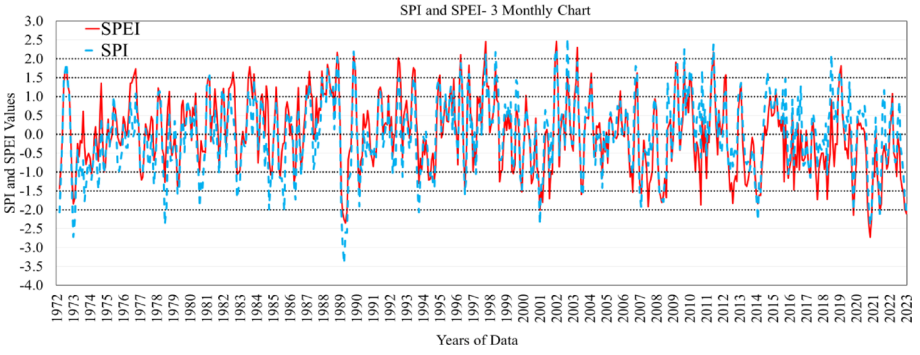



**Fig. 7** SPI and SPEI for 3 months

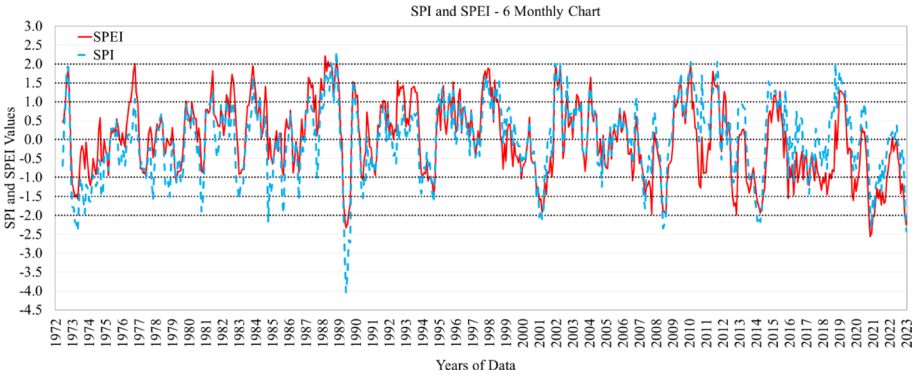



**Fig. 8** SPI and SPEI for 6 months

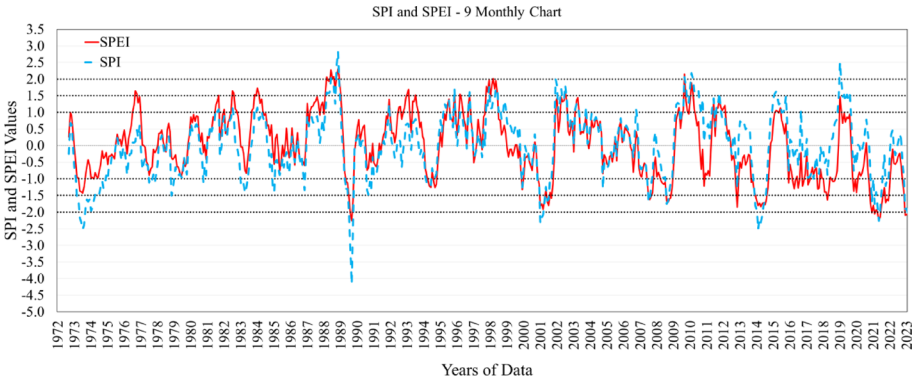



**Fig. 9** SPI and SPEI for 9 months

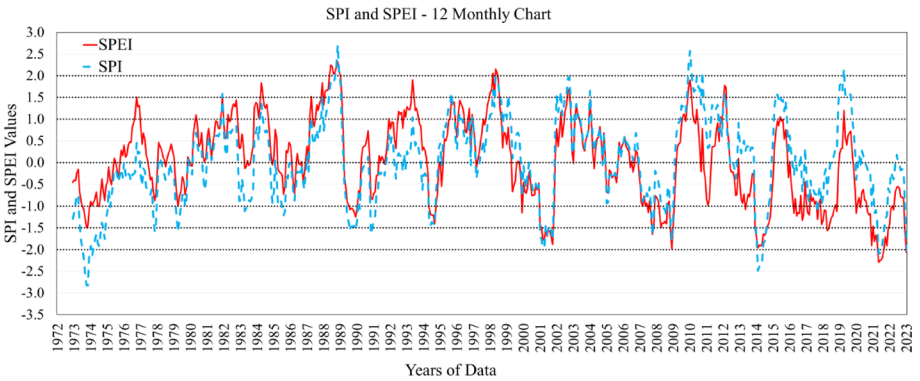



**Fig. 10** SPI and SPEI for 12 months

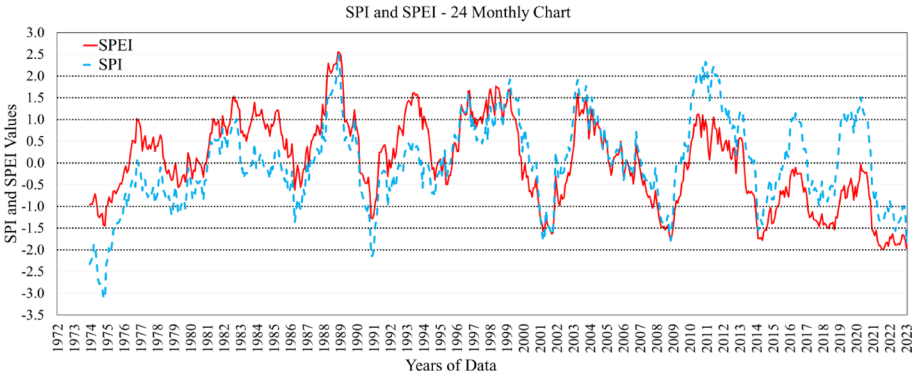



**Fig. 11** SPI and SPEI for 24 months

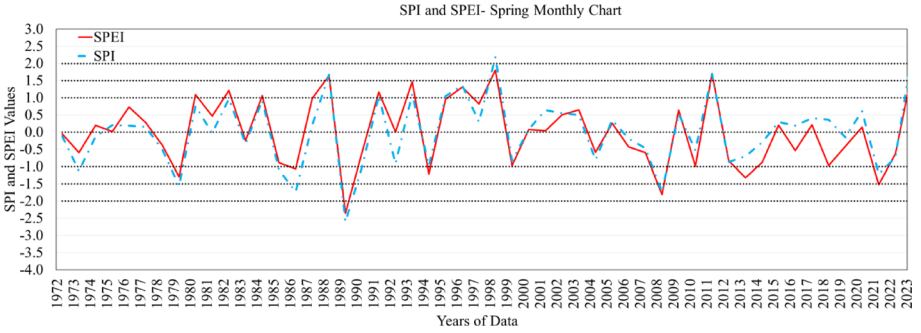



**Fig. 12** SPI and SPEI for spring season

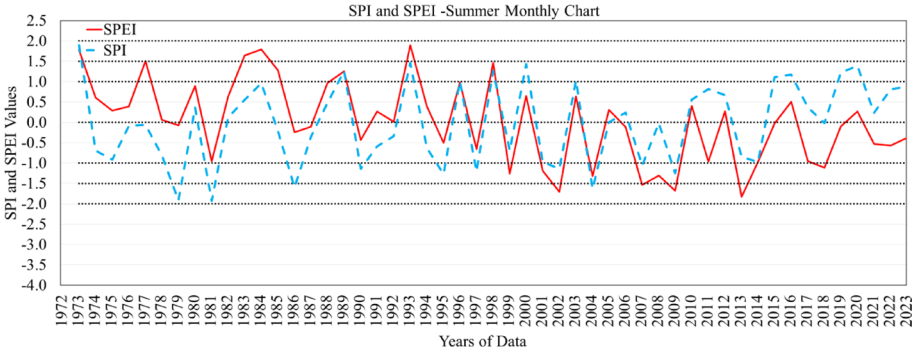



**Fig. 13** SPI and SPEI for summer season

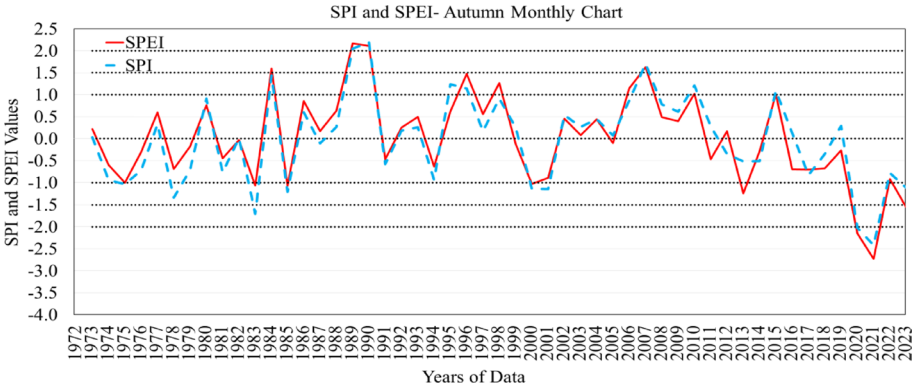



**Fig. 14** SPI and SPEI for autumn season

ture stress. The comparative assessment of these indices provides a conceptual basis for interpreting the drought characteristics presented in the following sections.

### 2.2.4 Mann Kendall test

The Mann–Kendall (MK) test is a non-parametric statistical method commonly used to identify the direction and significance of monotonic trends in hydroclimatic time series (Mann 1945; Kendall 1975). The MK test statistic (S) represents the difference between the number of positive and negative differences in the dataset and is calculated as follows:

$$\mathrm{S} = \sum_{i=1}^{n-1} \sum_{j=i+1}^{n} sign(x_i - x_j) \tag{25}$$

here $x_i$ and $x_j$ represent the sequential data values, n denotes the total number of observations, and sign refers to the sign function.

The sign function is calculated as follows:

$$sign(x_i - x_j) = \begin{cases} +1 \, if \; (x_i - x_j) > 0 \\ 0 \, if \; (x_i - x_j) = 0 \\ -1 \, if \; (x_i - x_j) < 0 \end{cases} \tag{26}$$

After calculating the MK test statistic (S), the variance of S is then computed.

$$Var \; (S) = \left[ n\,(n-1)\,(2n+1) - \sum_{t} \frac{t\,(t-1)\,(2t+5)}{18} \right] \tag{27}$$

Here, t represents the number of tied (repeated) values, and n denotes the total number of data points. Finally, the standard normal test statistic (Z) is calculated as follows (Hirsch et al. 1982; Yu et al. 1993; Berhail et al. 2022):

$$Z = \begin{cases} \frac{S-1}{\sqrt{Var(S)}} & if \ \ S > 0 \\ 0 & if \ \ S = 0 \\ \frac{S+1}{\sqrt{Var(S)}} & if \ \ S < 0 \end{cases} \tag{28}$$

The calculated Z values were interpreted in the context of climate change using the Mann–Kendall Z-value classification presented in Table 3 (Roy 2015).

## 3 Results

### 3.1 Results of temporal drought analysis based on SPI and SPEI

The 3-month SPI and SPEI values represent short-term meteorological droughts and exhibit frequent and abrupt fluctuations, particularly during transitional seasons. This indicates an increased risk of short-term drought events during critical periods for plant growth and agricultural production. The details of the 3 months drought indices are presented in the graph below (Fig. 7). In the analysis for the 1972–2023 period, extreme drought conditions were observed in September 1989, when the SPI dropped to approximately −3.5. In contrast, at the beginning of 2001, the SPI rose to around +2.8, reflecting an extremely wet period. In recent years, particularly between 2020 and 2021, although the SPI remained around −1.5, the SPEI dropped as low as −2.5, highlighting the role of temperature driven drought severity. In this context, the fact that SPEI values have become lower than SPI values since the 2000s demonstrates that rising temperatures have intensified evapotranspiration and significantly increased short-term drought severity.

The 6-month SPI and SPEI values are key indicators for assessing seasonal drought conditions, reflecting the periodic occurrence of drought and wet periods across Türkiye over time. Figure 8 presents the detailed drought index values obtained from the 6-month drought analysis. During the 1972–2023 period, particularly in late 1989, SPEI dropped to −2.0 and SPI declined to as low as −4.0, indicating the presence of extremely severe drought conditions. Similarly, in 1996 and 2001, both indices recorded values above +2.0, classifying these periods as severely wet. In recent years, especially toward 2023, SPEI values have

**Table 3** Classification of Mann–Kendall Z values (Dutta Roy 2015)

| Z Values | Significance of the trend |
|---|---|
| > 1.65 | Increasing trend at a confidence level greater than 90% |
| 1.64 to 0.84 | Increasing trend at a confidence level between 80% and 90% |
| 0.83 to 0.52 | Increasing trend at a confidence level between 70% and 80% |
| 0.52 to 0.00 | Increasing trend, statistically insignificant |
| 0.00 to − 0.52 | Decreasing trend, statistically insignificant |
| − 0.52 to − 0.83 | Decreasing trend at a confidence level between 70% and 80% |
| − 0.84 to − 1.64 | Decreasing trend at a confidence level between 80% and 90% |
| < − 1.65 | Decreasing trend at a confidence level greater than 90% |

notably dropped to around −2.5. Meanwhile, the SPI remained around −1.5 during the same period, further confirming that rising temperatures and their effect on evapotranspiration have intensified the severity of droughts at the seasonal scale.

The 9-month time scale allows for the assessment of medium-term climatic impacts on agriculture, water management, and ecosystems. As illustrated in Fig. 9, SPI reached its lowest level, approximately −4.5, in late 1989 marking one of the most extreme drought events observed during the study period. During the same period, SPEI also declined to around −3.0. Additionally, during the periods of 2014–2015 and 2020–2021, both indices recorded values below −2.0. The fact that SPEI values were lower than SPI during these intervals indicates that temperature-induced evaporation played a dominant role in shaping drought severity, even at the medium-term scale. On the other hand, in the positive peaks observed in 2001, SPI reached approximately+2.5, while SPEI remained around +2.0, reflecting periods of intense wetness.

The 12-month SPI and SPEI values serve as important indicators for evaluating the annual water balance and overall climatic trends. As shown in Fig. 10, annual drought patterns across Türkiye became particularly pronounced during the periods of 1989–1990, 2007–2008, 2014–2015, and 2020–2021, when both SPI and SPEI dropped to −2.0 or below. These periods represent critical phases during which meteorological drought began to transition into hydrological drought. The fact that SPEI values were consistently lower than SPI during these periods indicates that temperature-induced water losses have also intensified drought severity on an annual scale. In particular, the periods following 2007–2008 and post 2020 point to a transformative phase in which the influence of temperature became persistent and the nature of drought became increasingly complex.

The 24-month SPI and SPEI values are of critical importance for monitoring long-term climatic trends and hydrological drought. Analyses at this time scale reveal that drought is driven not only by precipitation deficits but also by evapotranspiration stress caused by rising temperatures. According to the results presented in Fig. 11, the periods of 1989–1991, 2007–2009, and 2020–2023 were characterized by values falling below −2,0 in both indices, indicating very severe and prolonged drought conditions. The consistently lower SPEI values compared to SPI after 2000 clearly demonstrate that elevated temperatures have further intensified long-term droughts. Notably, as of 2023, the continued low levels of both indices point to a persistent drought trend across Türkiye.

An evaluation of the temporal SPI and SPEI results for the period 1972–2023 reveals an increasing trend in both the frequency and severity of drought events across Türkiye. The recurrence of index values falling below −2,0 across all time scales particularly in 1989, 2007–2008, and the post 2020 period indicates the emergence of prolonged and large-scale drought conditions. The fact that SPEI consistently exhibits lower values than SPI highlights the systematic intensification of drought severity due to temperature-driven evapotranspiration. This trend suggests that, if temperature increases continue in the future, the likelihood of more frequent and intense temperature-induced droughts will increase across Türkiye.

## 3.2 Seasonal SPI and SPEI drought analysis results

### 3.2.1 Drought analysis results for the spring season

The SPI and SPEI values for the spring months between 1972 and 2023 indicate that drought and wetness conditions during this season across Türkiye have predominantly remained within the "near normal" range. The drought analyses based on spring precipitation and temperature data are presented graphically in Fig. 12. Additionally, detailed drought severity classifications for the spring season are shown in Table 4. In both indices, the most dominant class is "near normal," accounting for 67.31% in SPEI and 69.23% in SPI. However, in years such as 1989, 2008, and 2022, SPI and SPEI values dropped below −1.5, reaching the "severe drought" category most notably in 1989, when SPI fell below −2.0. During certain periods where the influence of temperature became more pronounced in the SPEI data (e.g., 2008–2010), the severity of drought was expressed with lower values in comparison to SPI, revealing that increased spring temperatures have intensified evapotranspiration and deepened the perception of drought.

According to the table data, drought conditions (including mild, severe, and extreme categories) occurred in 15.39% of cases based on SPEI and 15.38% based on SPI during the spring season. Although spring is generally favourable in terms of water balance, this finding indicates that the season still carries the risk of short-term droughts in certain years, which may negatively affect agricultural activities and early growth stages.

### 3.2.2 Drought analysis results for the summer season

The SPI and SPEI values for the summer season during the 1972–2023 period indicate that this season in Türkiye is more vulnerable to drought and more sensitive to the effects of temperature. Additionally, the graph illustrates that the divergence between SPI and SPEI curves has increased notably after 2000, particularly during summer, highlighting the grow-

**Table 4** Drought classification for the spring season

| | | SPEI | | SPI | |
|---|---|---|---|---|---|
| | | Frequency | Percentage (%) | Frequency | Percentage (%) |
| >2 | Extremely wet | 0 | 0.00 | 2 | 3.85 |
| 1.5 to 1.99 | Very wet | 4 | 7.69 | 2 | 3.85 |
| 1 to 1.49 | Moderately wet | 6 | 11.54 | 4 | 7.69 |
| − 0.99 to 0.99 | Near normal | 35 | 67.31 | 36 | 69.23 |
| − 1.00 to − 1.49 | Moderately dry | 4 | 7.69 | 4 | 7.69 |
| − 1.50 to − 1.99 | Severely dry | 2 | 3.85 | 3 | 5.77 |
| ≤ − 2 | Extremely dry | 1 | 1.92 | 1 | 1.92 |
| | | 52 | 100.00 | 52 | 100.00 |

ing influence of temperature on drought conditions (Fig. 13). These findings suggest that summer droughts, under the influence of climate change, are driven not only by precipitation deficits but also by increased evaporation triggered by high temperatures. This represents a critical warning for agricultural production and water management.

While SPI values are mostly concentrated in the "near normal" (57.69%) and "moderately wet" (21.15%) categories, SPEI values are more evenly distributed among the "severely dry" (7.69%), "moderately dry" (9.62%), and "very wet" (9.62%) classes (Table 5). This difference indicates that SPEI, which incorporates the effect of temperature, reflects drought conditions during summer as more severe and more variable. Notably, in years such as 2007, 2012, 2017, and 2021, SPEI dropped below −1.5 even when SPI showed positive values, revealing that temperature induced water deficits masked the impression of wetness.

### 3.2.3 Drought analysis results for the autumn season

The autumn SPI and SPEI data for the years 1972–2023 indicate that drought conditions during this season have generally been more favourable across Türkiye. However, notable drought and wetness anomalies have occurred periodically. As shown in the graph, particularly during the 2020–2023 period, both indices approached the −2.0 threshold, signalling a shift toward severe drought conditions and highlighting an increasing drought risk in autumn (Fig. 14).

According to the data in Table 6, "near normal" conditions dominate autumn, with a frequency of 67.31% for both SPI and SPEI. However, "moderately dry" conditions occurred in 11.54% of cases based on SPI and 9.62% based on SPEI. This difference suggests that SPI is more sensitive to precipitation deficits, while SPEI, by incorporating the effect of temperature, tends to produce more severe negative values in recent years. Notably, since 2016, both indices have more frequently exhibited negative values, indicating that the autumn season has become increasingly vulnerable to drought under the influence of climate change. This poses potential risks for the end of the agricultural season and water resources management.

**Table 5** Drought classification for the summer season

| | | SPEI | | SPI | |
|---|---|---|---|---|---|
| | | Frequency | Percentage (%) | Frequency | Percentage (%) |
| >2 | Extremely wet | 0 | 0.00 | 0 | 0.00 |
| 1.5 to 1.99 | Very wet | 5 | 9.62 | 1 | 1.92 |
| 1 to 1.49 | Moderately wet | 3 | 5.77 | 11 | 21.15 |
| − 0.99 to 0.99 | Near normal | 35 | 67.31 | 30 | 57.69 |
| − 1.00 to − 1.49 | Moderately dry | 5 | 9.62 | 6 | 11.54 |
| − 1.50 to − 1.99 | Severely dry | 4 | 7.69 | 4 | 7.69 |
| ≤ − 2 | Extremely dry | 0 | 0.00 | 0 | 0.00 |
| | | 52 | 100.00 | 52 | 100.00 |

**Table 6** Drought classification for the autumn season

| | | SPEI | | SPI | |
|---|---|---|---|---|---|
| | | Frequency | Percentage (%) | Frequency | Percentage (%) |
| >2 | Extremely wet | 2 | 3.85 | 2 | 3.85 |
| 1.5 to 1.99 | Very wet | 2 | 3.85 | 1 | 1.92 |
| 1 to 1.49 | Moderately wet | 5 | 9.62 | 5 | 9.62 |
| − 0.99 to 0.99 | Near normal | 35 | 67.31 | 35 | 67.31 |
| − 1.00 to − 1.49 | Moderately dry | 5 | 9.62 | 6 | 11.54 |
| − 1.50 to − 1.99 | Severely dry | 1 | 1.92 | 1 | 1.92 |
| ≤ − 2 | Extremely dry | 2 | 3.85 | 2 | 3.85 |
| | | 52 | 100.00 | 52 | 100.00 |

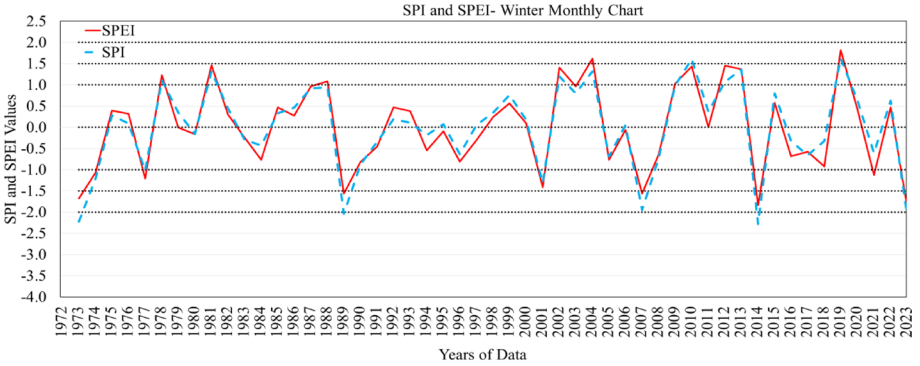



**Fig. 15** SPI and SPEI for winter season

### 3.2.4 Drought analysis results for the winter season

The SPI and SPEI values for the winter season during the 1972–2023 period indicate that drought conditions across Türkiye have generally remained at a moderate level during this season. As illustrated in Fig. 15, both indices approached the −2.0 threshold in the winters of 1989, 2008, and 2023, indicating the presence of severe drought conditions during those years.

According to the data in Table 7, "near normal" conditions prevailed in the winter season with a frequency of 68.63% for SPI and 62.75% for SPEI. However, "moderately wet" conditions were observed in 15.69% of the cases based on SPEI and 11.76% based on SPI. This suggests that, in certain years, winter provided a short-term recovery in terms of precipitation, yet this improvement was more limited when assessed through SPEI, which accounts for temperature effects. In years such as 2014, 2017, and 2023, the fact that SPEI recorded

**Table 7** Drought classification for the winter season

| | | SPEI | | SPI | |
|---|---|---|---|---|---|
| | | Frequency | Percentage (%) | Frequency | Percentage (%) |
| >2 | Extremely wet | 0 | 0.00 | 0 | 0.00 |
| 1.5 to 1.99 | Very wet | 2 | 3.92 | 2 | 3.92 |
| 1 to 1.49 | Moderately wet | 8 | 15.69 | 6 | 11.76 |
| − 0.99 to 0.99 | Near normal | 32 | 62.75 | 35 | 68.63 |
| -1.00 to -1.49 | Moderately dry | 4 | 7.84 | 3 | 5.88 |
| -1.50 to -1.99 | Severely dry | 5 | 9.80 | 1 | 1.96 |
| ≤-2 | Extremely dry | 0 | 0.00 | 4 | 7.84 |
| | | 51 | 100.00 | 51 | 100.00 |

**Table 8** Seasonal correlation between SPI and SPEI

| Correlation/ determination coefficient | Spring | Summer | Autumn | Winter |
|---|---|---|---|---|
| r | 0.9158 | 0.5771 | 0.9290 | 0.9666 |
| $R^2$ | 0.8386 | 0.3331 | 0.8631 | 0.9343 |

lower values than SPI demonstrates that temperature has also intensified drought conditions during winter. Particularly over the past decade, the tendency of SPEI to shift toward negative values indicates that winter droughts in Türkiye are driven not only by precipitation deficits but also by above-normal temperatures. This has potential implications for snow cover, soil moisture, and the recharge of reservoirs.

Seasonal analyses based on SPI and SPEI data from the 1972–2023 period reveal that. although drought events across Türkiye have largely occurred under “near normal” conditions, moderate to severe droughts have periodically affected all seasons. The fact that SPEI yields lower values than SPI particularly in summer and autumn demonstrates that rising temperatures have intensified drought severity through increased evapotranspiration, and that this effect plays a critical role in the seasonal distribution of drought. Summer has emerged as the season in which temperature induced drought is felt most intensely, whereas winter has shown relatively more moderate conditions. In recent years, especially since 2000, both the trends observed in the graphs and the distribution of drought categories indicate increasing climatic instability and the emergence of a more complex pattern of seasonal drought across the country.

The correlation and determination coefficients illustrating the relationship between the SPEI and SPI drought indices at both seasonal and long-term scales are presented in Tables 8 and 9. Additionally, the visualization of the correlation between SPI and SPEI results is given in Figs. 16 and 17. At the seasonal scale, the highest correlation coefficient was observed during the winter season ($r$=0.9666; $R^2$ = 0.9343). This can be explained by the fact that evaporation and evapotranspiration processes are at minimal levels during

**Table 9** Temporal scale relationship between SPI and SPEI

| Correlation/ Determination coefficient | 3 Months | 6 Months | 9 Months | 12 Months | 24 Months |
|---|---|---|---|---|---|
| r | 0.8598 | 0.8292 | 0.8197 | 0.8036 | 0.7106 |
| $R^2$ | 0.7394 | 0.6875 | 0.6719 | 0.6458 | 0.5049 |

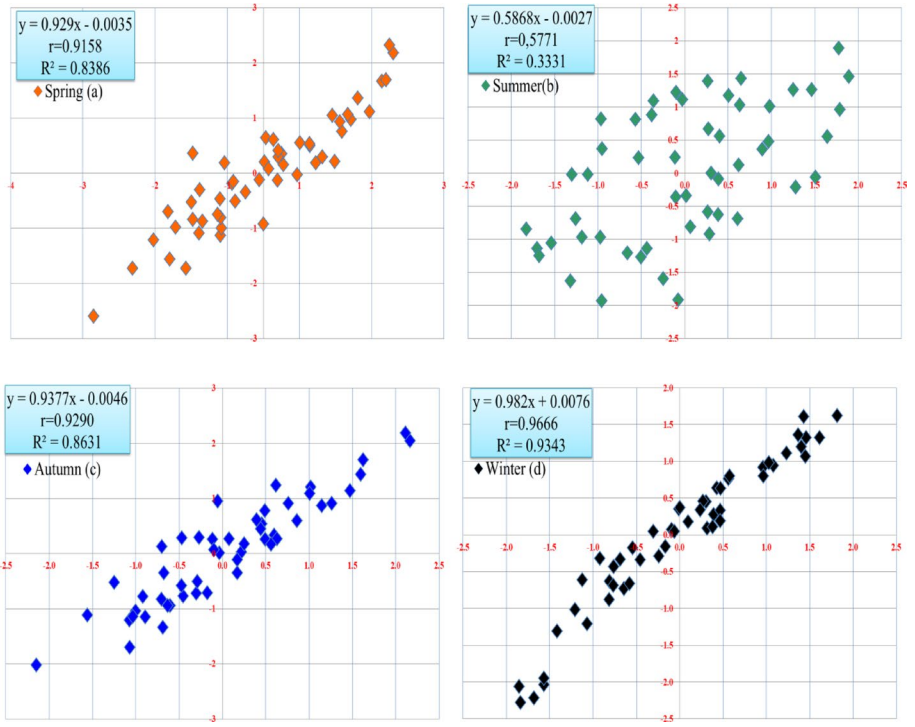



**Fig. 16** Corelation of seasonal SPI and SPEI results (a-b-c-d)

winter, resulting in SPI and SPEI producing largely similar hydroclimatic signals. Similarly, strong relationships were also observed in autumn ($r$=0.9290; $R^2$ = 0.8631) and spring ($r$=0.9158; $R^2$ = 0.8386). Although the influence of evapotranspiration increases during these seasons, they are generally dominated by precipitation, allowing SPI and SPEI to represent drought conditions in a relatively consistent manner.

In contrast, the correlation significantly decreases during the summer season ($r$=0.5771; $R^2$ = 0.3331). This weak relationship can be attributed to the fact that, during summer, rising temperatures lead to high levels of potential evapotranspiration, causing the SPI which is based solely on precipitation to inadequately represent actual drought conditions. By accounting for potential evapotranspiration, SPEI provides more sensitive and realistic assessments, particularly in the evaluation of agricultural and atmospheric drought.

An evaluation of the results at the temporal scale reveals that the correlation between SPI and SPEI is quite strong at short-term time scales (3 and 6 months), with correlation coefficients ranging from $r$=0.8598 to 0.8292 and coefficients of determination ($R^2$) ranging from

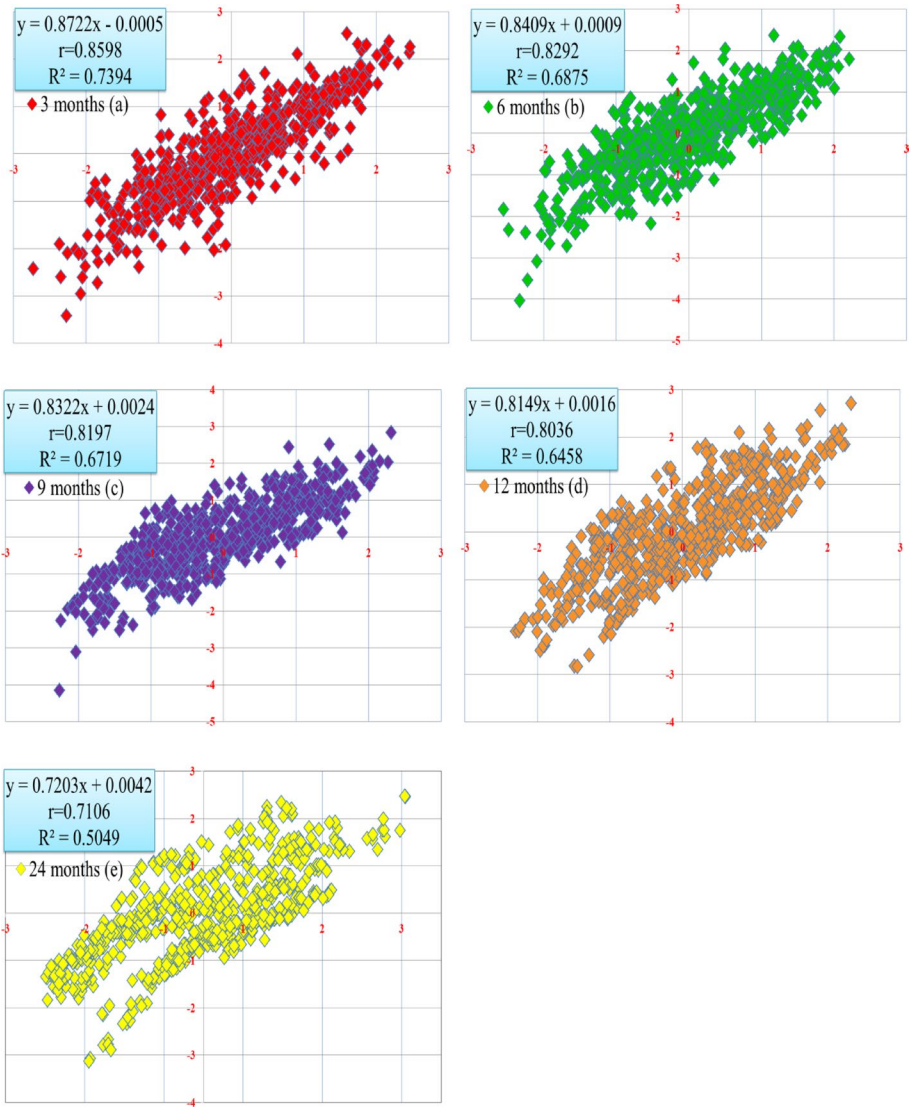
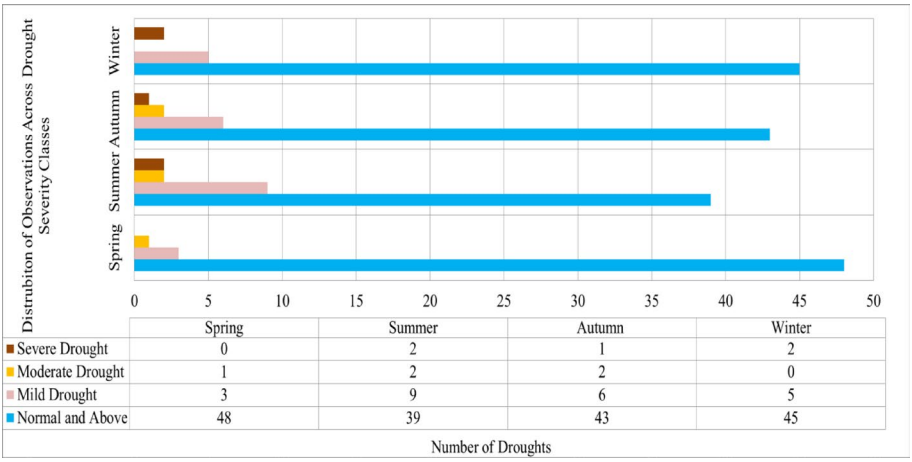



**Fig. 17** Corelation of temporal SPI and SPEI results (a-b-c-d-e)

0.7394 to 0.6875. This finding indicates that precipitation is the dominant factor in short-term hydroclimatic anomalies, while evapotranspiration plays a relatively limited role.

However, as the time scale increases particularly at 9-, 12-, and 24-months intervals a notable decline in correlation values is observed (e.g., at the 24-month scale, $r$=0.7106; $R^2$ = 0.5049). This decline indicates that long-term droughts are shaped not only by precipitation deficits but also by increased evapotranspiration driven by rising temperatures. In this context, SPEI can be considered a more comprehensive tool for drought assessment, as it accounts for both inputs (precipitation) and outputs (evapotranspiration) in the water balance.




| | Spring | Summer | Autumn | Winter |
|---|---|---|---|---|
| Severe Drought | 0 | 2 | 1 | 2 |
| Moderate Drought | 1 | 2 | 2 | 0 |
| Mild Drought | 3 | 9 | 6 | 5 |
| Normal and Above | 48 | 39 | 43 | 45 |

**Fig. 18** PNI seasonal drought distribution

### 3.3 Seasonal PNI drought analysis results

The seasonal drought assessment based on the Normalized Precipitation Index (PNI) reveals the distribution of meteorological drought events across Türkiye for different seasons. According to the updated analysis, summer remains the most drought-prone season, with a total of 13 drought events, including 2 classified as severe and 2 as moderate. This confirms that summer is particularly vulnerable to precipitation deficits, likely due to increased evapotranspiration and decreased rainfall. Conversely, spring exhibited the most stable conditions, with 48 out of 52 years falling under the "normal and above" category and no severe drought occurrences, indicating a more resilient hydrometeorological pattern. Autumn and winter displayed intermediate characteristics. Autumn experienced 9 drought seasons, predominantly of mild and moderate severity, while winter recorded 7 drought events, including 2 severe but no moderate cases. Overall, the PNI results suggest that meteorological droughts in Türkiye are more frequent during the warmer part of the year, particularly summer, whereas transitional (spring, autumn) and colder seasons show relatively lower drought severity. These findings emphasize the need for season-specific drought monitoring and adaptation strategies, particularly focusing on summer vulnerability. The results are visualized in Fig. 18.

The seasonal drought results obtained from the PNI method are generally consistent with those derived from the SPI and SPEI indices. In particular, summer emerges as the most drought-prone season across all three indices. While the PNI analysis identified 13 drought events during the summer, the SPI and SPEI results also revealed significant negative anomalies and elevated drought severity during this period. Moreover, SPEI values in summer exhibited deeper negative deviations compared to SPI, which reinforces the PNI indicated drought frequency by highlighting the amplifying effect of temperature-induced evapotranspiration. Spring, identified by the PNI as the most climatically stable season with the fewest drought events, was also characterized by predominantly positive or near-normal values in SPI and SPEI analyses. Autumn and winter, in turn, showed intermediate drought severity across all three indices, without reaching the extreme levels observed in summer. This com-

parative evaluation confirms that the detailed temporal sensitivity of SPI and SPEI aligns well with the general trends captured by PNI, underscoring the added value of multi-index approaches in improving the robustness and reliability of seasonal drought assessments.

### 3.4 Mann Kendal test results

According to the Mann–Kendall (MK) trend analysis, the SPI and SPEI indices across Türkiye exhibit varying tendencies on both annual and seasonal scales (Table 1). At the 12-month time scale, the SPEI value (–0.05) indicates an insignificant decreasing trend, while the SPI value (0.03) shows an insignificant increasing trend. This suggests that, over the long term, drought trends do not display a statistically significant direction but that temperature variations may periodically intensify drought severity.

In the spring season, the SPI shows an increasing trend (0.67) at a 70–80% confidence level, whereas the SPEI reveals a decreasing trend (–1.15) at an 80–90% confidence level. This divergence highlights that temperature increases enhance evapotranspiration during spring, thereby amplifying drought conditions and demonstrating the higher temperature sensitivity of the SPEI index.

During summer, the SPI exhibits a statistically significant increasing trend (1.98) above the 90% confidence level, while the SPEI displays a strong decreasing trend (–3.51) with the same level of significance. This contrast indicates that elevated temperatures and increased evapotranspiration dominate summer drought dynamics, offsetting the influence of occasional rainfall increases.

During winter, the SPI value (0.64) indicates an increasing trend at the 70–80% confidence level, and the SPEI value (0.23) also reveals a weakly increasing but statistically insignificant trend. These results imply that winter months have shown a slight wetting tendency, mainly due to enhanced precipitation and reduced evapotranspiration under low-temperature conditions. However, the lack of statistical significance suggests that the observed positive tendency may represent short-term variability rather than a persistent long-term trend.

In autumn, the SPI value (0.22) indicates a weakly increasing but statistically insignificant trend, while the SPEI value (–1.57) shows a decreasing trend at the 80–90% confidence level. This contrast suggests that, although precipitation-based conditions remain relatively stable, temperature-induced evapotranspiration has intensified in recent decades, leading to a weakening of moisture availability during the autumn months. The negative SPEI signal highlights that warming has begun to offset the effects of autumn rainfall, increasing the likelihood of dry-end growing seasons.

Overall, the results reveal a clear intensification and temporal clustering of drought events across Türkiye since the early 2000s at both seasonal and annual time scales. The Mann–Kendall analysis indicates that while precipitation-based indices (SPI and PNI) generally exhibit weak positive or near-neutral trends, the temperature-sensitive SPEI shows notable negative trends across much of the country. This contrast highlights the increasing role of temperature-induced evapotranspiration in shaping long-term drought behavior beyond precipitation deficits alone. The divergence between indices is most pronounced during summer and autumn, whereas relatively weaker or opposite tendencies in winter suggest that rising temperatures increasingly redefine the seasonal drought regime at the national scale.

## 4 Discussion

The differences in drought severity identified by the three indices are primarily driven by their input variables and sensitivity to temperature. Because SPI and PNI are precipitation-only metrics, they reflect short-term rainfall anomalies but can underestimate drought under warming conditions. In contrast, SPEI incorporates the moisture balance (P − PET), making it more responsive to heat- and evapotranspiration-driven deficits hence stronger and more persistent drought signals than SPI/PNI in warmer and drier years. The identified drought periods correspond closely with the years exhibiting negative precipitation anomalies and positive temperature anomalies, as illustrated in Figs. 2, 3, 4 and 5. These climatic anomalies collectively explain the temporal clustering and intensity of drought events observed across Türkiye. While not the purpose of this study and does not include a formal attribution analysis, the consistent co-occurrence of warming trends and increased drought frequency provides observational evidence of the influence of climate variability consistent with climate change patterns observed in the country.

These findings are consistent with recent drought studies conducted across Türkiye, which report similar sensitivities of precipitation- and temperature-based drought indices. In particular, the nationwide study by Yaman Öz et al. (2024), which included data from 219 stations, revealed that between 1991 and 2022, not only declining precipitation but also increasing temperatures contributed to higher frequency and severity of meteorological drought. This finding aligns with this study results, especially the observation that SPEI values were lower than SPI values during summer and autumn, clearly confirming the impact of thermal drought during the warmer months. Additionally, the study by Gumus (2023) supports this trend, as it showed that since the 1990s, SPEI has identified moderate and severe drought events more frequently than SPI at the 3, 6, and 12-month time scales. These findings confirm that temperature-driven evapotranspiration intensifies the perception and severity of drought.

At the national and regional scale, several recent studies further corroborate the increasing role of temperature-driven drought processes identified in this study. (Serkendiz et al. 2024). Extending beyond SPI/SPEI, a multi-index comparison (SPI, SPEI, RDI; 219 stations) found region-dependent sensitivities and highlighted the added value of PET-aware metrics, echoing our rationale for a multi-index framework (Öz et al. 2024). Complementary evidence from remote sensing–aided assessments over Türkiye also confirms recent intensification and spatial shifts in drought conditions, supporting nationwide signals obtained from this study (Khorrami and Gündüz 2022). Finally, projection-based work focusing on Türkiye located in Mediterranean basin indicates stronger future drying under climate change, reinforcing interpretation in this study that warming-driven evapotranspiration contributes to the observed post-2000 anomalies (Erkol et al. 2024).

Taken together, the seasonal and annual coherence between SPI, PNI, and SPEI highlights the robustness of the adopted multi-index framework. This methodological structure not only enhances the interpretation of drought variability in Türkiye but also provides a replicable approach for comparative drought monitoring in other semi-arid and climatically heterogeneous regions.

Despite the advantages of the adopted multi-index approach, this study is limited to SPI, SPEI, and PNI and does not incorporate other widely used drought indices such as the reconnaissance drought index (RDI) or Self-Calibrated Palmer Drought Severity Index (scPDSI).

The exclusion of these indices represents a methodological limitation of the present analysis. While RDI and scPDSI can provide valuable insights into soil moisture dynamics and longer-term hydrological drought processes, their application requires additional data inputs and assumptions that were beyond the scope of this nationwide, long-term assessment. Consequently, the results presented here primarily reflect meteorological drought conditions and temperature-driven moisture deficits, and future studies could benefit from integrating additional drought indices to further improve the characterization of drought processes across Türkiye.

Regarding the estimation of atmospheric water demand, potential evapotranspiration (PET) in this study was calculated using the Thornthwaite method. Although this approach enables long-term and spatially consistent PET estimation across all stations, it represents a limitation under warming climate conditions, as it may underestimate atmospheric evaporative demand compared to physically based methods. Consequently, the magnitude of SPEI values and the intensity of temperature-driven droughts may be affected. Future studies could reduce this uncertainty by incorporating alternative PET formulations or complementary data sources where additional meteorological variables are available.

Another methodological consideration concerns the probabilistic formulation of SPI, which in this study is based on the two-parameter Gamma distribution. However, the assumption of a single parametric distribution represents a limitation, particularly for climatically heterogeneous regions such as Türkiye. Different probability distributions may provide varying representations of precipitation behavior at local or basin scales, potentially influencing drought classification. While the use of areal precipitation averages reduces local variability, future studies could benefit from testing alternative distributions to further assess the sensitivity of SPI-based drought estimates.

From a spatial perspective, the use of data from 255 meteorological stations provides a strong observational basis for national-scale drought assessment, although spatial representativeness may vary regionally. In addition, the Ordinary Kriging interpolation approach, while effective in generating spatially continuous precipitation fields, may smooth localized extremes and introduce interpolation-related uncertainty. Furthermore, the exclusive reliance on in-situ observations represents a limitation, as complementary remote sensing products (e.g., soil moisture or vegetation-based indicators) could provide additional insights into spatial drought variability. Future studies could integrate ground-based and satellite-derived datasets to further enhance spatial robustness and reduce uncertainty in drought characterization.

More broadly, climate-based research on precipitation variability and rising temperatures in Türkiye confirms the growing prevalence of temperature-induced droughts over time. While future drought projections are beyond the scope of the present study, the findings provide an essential historical context for sustainable water resource management. The identification of long-term drought patterns across multiple temporal scales establishes a baseline for evaluating future risks under changing climatic conditions. Understanding the temporal variability and recurrence of past droughts supports more informed decision-making in drought preparedness, agricultural product planning, and water allocation policies. Therefore, historical drought analysis serves as a crucial input for adaptive management and the development of long-term water governance strategies in Türkiye.

Consistent with these findings, drought intensity in Türkiye has clearly shifted toward more persistent and temperature-driven events after 2000, indicating a regime change rather

than isolated dry years. The Mann–Kendall trend analysis supports the temporal findings by confirming that drought severity has intensified since the early 2000s, particularly during the summer months, where statistically significant negative trends in SPEI reflect dominant temperature and evapotranspiration effects. In contrast, weak positive trends in winter indicate that precipitation increases may provide only temporary relief under continuing warming conditions. These opposing seasonal trends underline the emergence of a more complex and temperature-sensitive drought regime in Türkiye, consistent with the observed Mediterranean-wide drying tendency.

## 5 Conclusion

This study presents a comprehensive assessment of temporal drought dynamics in Türkiye through a multi-dimensional approach, using long-term precipitation and temperature data from the 1972–2023 period and applying the SPI, SPEI, and PNI indices. The findings indicate that, overall, drought events have predominantly clustered within the "near normal" category. However, during the periods of 1989–1991, 2007–2009, and 2020–2023, the frequency and intensity of severe and extreme droughts significantly increased. The fact that SPEI values were lower than SPI values during these periods points to the intensifying effect of rising temperatures and associated evapotranspiration on drought severity. Notably, in summer, SPEI values dropped below − 1.5, indicating the occurrence of very severe drought conditions. The PNI results further supported this trend, identifying 13 severe drought seasons in summer, whereas in spring and winter, the proportion of "normal and above" conditions reached high levels 88.5% and 82.3%, respectively.

Türkiye is entering a temperature-driven drought regime marked by intensified seasonal contrasts and persistent aridity, underscoring the urgent need to integrate temperature effects into national drought monitoring and adaptation strategies.

These multi scale analyses demonstrate that while SPI and PNI, as precipitation-based indices, are sufficient for identifying meteorological drought, SPEI by incorporating temperature effects reveals a deeper structure of drought, particularly during the summer and autumn seasons. Therefore, employing a multi-index approach that combines both precipitation and temperature-based indices provide a more accurate and comprehensive assessment of drought risks under climate change. This study offers a scientific basis for the development of national drought monitoring systems and supports decision-making in agricultural planning, water resources management, and climate adaptation policies. Results obtained in the present study shows that if temperature increases continue in the future, the likelihood of more frequent and intense temperature induced droughts will increase across Türkiye.

By integrating temperature-based drought indicators, basin-scale water management, and climate-smart agriculture, Türkiye can safeguard its food and water security under a warming climate. A coordinated national framework linking science, technology and policy could transform drought from a recurring crisis into a manageable climate problem.

Specifically, it is recommended that the Turkish State Meteorological Service (TSMS) integrate temperature anomalies into national drought early-warning systems, while the General Directorate of State Hydraulic Works (DSİ) utilize spatial and temporal drought assessments to align long-term water allocation and reservoir operations with drought-adaptive management strategies.

**Author contributions** All authors contributed to the study design and conceptualization. Bülent Selek: Data precipitation, Writing-Review and Editing, Methodology. Murat Pinarlik: Formal analysis, Writing–original draft, Visualization. Ismail Faki: Formal analysis, Methodology, Visualization, Writing–original draft. Zeliha Selek: Supervising, Writing-Review and Editing.

**Funding** Open access funding provided by the Scientific and Technological Research Council of Türkiye (TÜBİTAK). The authors declare that no funds, grants, or other support were received during the preparation of this manuscript.

**Data availability** The precipitation and temperature datasets used in this study were obtained from the Turkish State Meteorological Service (TSMS) and are not publicly available due to institutional data access restrictions. Processed and aggregated data generated during the current study are available from the corresponding author upon reasonable request.

## Declarations

**Conflict of interest** The authors declare that they have no competing interests.

**Ethical approval** Not applicable.

**Consent to participate** Not applicable.

**Consent for publication** Not applicable.

**Open Access** This article is licensed under a Creative Commons Attribution 4.0 International License, which permits use, sharing, adaptation, distribution and reproduction in any medium or format, as long as you give appropriate credit to the original author(s) and the source, provide a link to the Creative Commons licence, and indicate if changes were made. The images or other third party material in this article are included in the article's Creative Commons licence, unless indicated otherwise in a credit line to the material. If material is not included in the article's Creative Commons licence and your intended use is not permitted by statutory regulation or exceeds the permitted use, you will need to obtain permission directly from the copyright holder. To view a copy of this licence, visit http://creativecommons.org/licenses/by/4.0/.

## References

Abramowitz M, Stegun A (1965) Handbook of mathematical functions. Dover, New York

Aksu H, Cavus Y, Aksoy H, Akgül MA, Turker S, Eris E (2022) Spatiotemporal analysis of drought by CHIRPS precipitation estimates. Theor Appl Climatol 148:517–529. https://doi.org/10.1007/s00704-022-03960-6

Berhail S, Tourki M, Merrouche I, Bendekich H (2022) Geo-statistical assessment of meteorological drought in the context of climate change: case of the Macta basin (Northwest of Algeria). Model Earth Syst Environ 8(13). https://doi.org/10.1007/s40808-020-01055-7

Cebeci İ, Demirkıran O, Doğan O, Karagöz Sezer K, Öztürk Ö, Elbaşı F (2019) Drought assessment of Turkey based on the provinces. Toprak Su Dergisi 169–176. https://doi.org/10.21657/topraksu.655613

Ceyhunlu AI, Ceribasi G (2024a) Prediction of precipitation–temperature data and drought assessment of Turkey with stochastic time series models. Pure Appl Geophys 181:2913–2933. https://doi.org/10.1007/s00024-024-03559-0

Ceyhunlu AI, Ceribasi G (2024b) Changes in precipitation and air temperature over Turkey using innovative trend Pivot analysis method. J Water Clim Change 15(5):2446–2463. https://doi.org/10.2166/wcc.2024.041

Cui A, Li J, Zhou Q, Zhu H, Liu H, Yang C, Wu G, Li Q (2024) Propagation dynamics from meteorological drought to grace-based hydrological drought and its influencing factors. Remote Sens 16(6):976. https://doi.org/10.3390/rs16060976

Danandeh Mehr A, Vaheddoost B (2020) Identification of the trends associated with the SPI and SPEI indices across Ankara, Turkey. Theor Appl Climatol 139:1531–1542. https://doi.org/10.1007/s00704-019-03071-9

Dikshit A, Pradhan B, Alamri AM (2021) Long lead time drought forecasting using lagged climate variables and a stacked long short-term memory model. Sci Total Environ 755:142638. https://doi.org/10.1016/j.scitotenv.2020.142638

Dutta Roy A (2015) Trend detection in temperature and rainfall over Rajasthan during the last century. Asian J Res Soc Sci Humanit 5(12). https://doi.org/10.5958/2249-7315.2015.00022.2

Erkol ZI, Yesilyurt SN, Dalkilic HY (2024) Impacts of climate change on Spatial drought distribution in the mediterranean basin (Turkey): different climate models and downscaling methods. Theor Appl Climatol 155:4065–4087. https://doi.org/10.1007/s00704-024-04867-0

Fan J, Wu L, Zhang F, Cai H, Wang X, Lu X, Xiang Y (2018) Evaluating the effect of air pollution on global and diffuse solar radiation prediction using support vector machine modeling based on sunshine duration and air temperature. Renew Sustain Energy Rev 94:732–747. https://doi.org/10.1016/j.rser.2018.06.029

Farahmand A, AghaKouchak A (2015) A generalized framework for deriving nonparametric standardized drought indicators. Adv Water Resour 76:140–145. https://doi.org/10.1016/j.advwatres.2014.11.012

Ghozat A, Sharafati A, Hosseini SA (2022) Satellite-based monitoring of meteorological drought over different regions of iran: application of the CHIRPS precipitation product. Environ Sci Pollut Res 29:36115–36132. https://doi.org/10.1007/s11356-022-18773-3

Gumus V (2023) Evaluating the effect of the SPI and SPEI methods on drought monitoring over Turkey. J Hydrol 626:130386. https://doi.org/10.1016/j.jhydrol.2023.130386

Guttman NB (1999) Accepting the standardized precipitation index: a calculation algorithm. J Am Water Resour Assoc 35(2):311–322. https://doi.org/10.1111/j.1752-1688.1999.tb03592.x

Ha TV, Uereyen S, Kuenzer C (2023) Agricultural drought conditions over Mainland Southeast Asia: spatiotemporal characteristics revealed from MODIS-based vegetation time-series. Int J Appl Earth Obs Geoinf 121:103378. https://doi.org/10.1016/j.jag.2023.103378

Hassan MA, Khalil A, Kaseb S, Kassem MA (2017) Exploring the potential of tree-based ensemble methods in solar radiation modeling. Appl Energy 203:897–916. https://doi.org/10.1016/j.apenergy.2017.06.104

Hirsch RM, Slack JR, Smith RA (1982) Techniques of trend analysis for monthly water quality data. Water Resour Res 18:107–121. https://doi.org/10.1029/WR018i001p00107

Homdee T, Pongput K, Kanae S (2016) A comparative performance analysis of three standardized Climatic drought indices in the Chi river basin. Thail Agric Nat Resour 50:211–219. https://doi.org/10.1016/j.anres.2016.02.002

Kendall MG (1975) Rank correlation methods. Griffin, London

Khorrami B, Gündüz O (2022) Detection and analysis of drought over Turkey with remote sensing and model-based drought indices. Geocarto Int 37(26):12171–12193. https://doi.org/10.1080/10106049.2022.2066197

Kumar R, Aggarwal RK, Sharma JD (2015) Comparison of regression and artificial neural network models for estimation of global solar radiations. Renew Sustain Energy Rev 52:1294–1299. https://doi.org/10.1016/j.rser.2015.08.021

Lee S, Moriasi DN, Danandeh Mehr A, Mirchi A (2024) Sensitivity of standardized precipitation and evapotranspiration index (SPEI) to the choice of SPEI probability distribution and evapotranspiration method. J Hydrol Reg Stud 53:101761. https://doi.org/10.1016/j.ejrh.2024.101761

Liu S, Kang W, Wang T (2016) Drought variability in inner Mongolia of Northern China during 1960–2013 based on standardized precipitation evapotranspiration index. Environ Earth Sci 75(2):145. https://doi.org/10.1007/s12665-015-4996-0

Liu X, Yu S, Yang Z, Dong J, Peng J (2024) The first global multi-timescale daily SPEI dataset from 1982 to 2021. Sci Data 11:223. https://doi.org/10.1038/s41597-024-03047-z.

Mahmoudi P, Rigi A, Miri Kamak M (2019) A comparative study of precipitation-based drought indices with the aim of selecting the best index for drought monitoring in Iran. Theor Appl Climatol 137(3–4):3123–3138. https://doi.org/10.1007/s00704-019-02778-z

Mann HB (1945) Nonparametric tests against trend. Econometrica 13:245–259

Mavromatis T (2007) Drought index evaluation for assessing future wheat production in Greece. Int J Climatol 27(7):911–924. https://doi.org/10.1002/joc.1449

McKee TB, Doesken NJ, Kleist J (1993) The relationship of drought frequency and duration to time scales. In: Proceedings of the 8th conference on applied climatology, Boston, MA, USA. pp 179–183

Meseguer-Ruiz O, Serrano-Notivoli R, Aránguiz-Acuña A, Fuentealba M, Nuñez-Hidalgo I, Sarricolea P, Garreaud R (2024) Comparing SPI and SPEI to detect different precipitation and temperature regimes in Chile throughout the last four decades. Atmos Res 297:107085. https://doi.org/10.1016/j.atmosres.2023.107085

Mokhtar A, Jalali M, He H, Al-Ansari N, Elbeltagi A, Alsafadi K, Abdo HG, Sammen SS, Gyasi-Agyei Y, Rodrigo-Comino J (2021) Estimation of SPEI meteorological drought using machine learning algorithms. IEEE Access 9:65503–65523. https://doi.org/10.1109/ACCESS.2021.3074305

Moreno A, Gilabert MA, Martínez B (2011) Mapping daily global solar irradiation over spain: a comparative study of selected approaches. Sol Energy 85(9):2072–2084. https://doi.org/10.1016/j.solener.2011.05.017

Nwayor IJ, Robeson SM (2024) Exploring the relationship between SPI and SPEI in a warming world. Theor Appl Climatol 155:2559–2569. https://doi.org/10.1007/s00704-023-04764-y

Ojha SS, Singh V, Roshni T (2021) Comparison of meteorological drought using SPI and SPEI. Civ Eng J 7(12). https://doi.org/10.28991/cej-2021-03091783

Ortiz–Gómez R, Flowers–Cano RS, Medina–García G (2022) Sensitivity of the RDI and SPEI drought indices to different models for estimating evapotranspiration potential in semiarid regions. Water Resour Manag 36:2471–2492. https://doi.org/10.1007/s11269-022-03154-9

Öz FY, Özelkan E, Tatlı H (2024) Comparative analysis of SPI, SPEI, and RDI indices for assessing spatio-temporal variation of drought in Türkiye. Earth Sci Inf 17:4473–4505. https://doi.org/10.1007/s12145-024-01401-8

Palmer DS (1965) Sequencing jobs through a multi-stage process in the minimum total time—a quick method of obtaining a near pptimum. J Oper Res Soc 16:101–107. https://doi.org/10.1057/jors.1965.8

Papadopoulos S, Azar E, Woon WL, Kontokosta CE (2018) Evaluation of tree-based ensemble learning algorithms for Building energy performance Estimation. J Build Perform Simul 11(3):322–332. https://doi.org/10.1080/19401493.2017.1354919

Pei Z, Fang S, Wang L, Yang W (2020) Comparative analysis of drought indicated by the SPI and SPEI at various timescales in inner Mongolia, China. Water 12:1925. https://doi.org/10.3390/w12071925

Pieper P, Düsterhus A, Baehr J (2020) A universal standardized precipitation index candidate distribution function for observations and simulations. Hydrol Earth Syst Sci 24(9):4541–4565. https://doi.org/10.5194/hess-24-4541-2020

Politi N, Vlachogiannis D, Sfetsos A, Nastos PT, Dalezios NR (2022) High resolution future projections of drought characteristics in Greece based on SPI and SPEI indices. Atmosphere 13:1468. https://doi.org/10.3390/atmos13091468

Quej VH, Almorox J, Arnaldo JA, Saito L (2017) ANFIS, SVM and ANN soft-computing techniques to estimate daily global solar radiation in a warm sub-humid environment. J Atmos Sol -Terr Phys 155:62–70. https://doi.org/10.1016/j.jastp.2017.02.002

Rawat S, Ganapathy A, Agarwal A (2022) Drought characterization over Indian sub-continent using GRACE-based indices. Sci Rep 12:15432. https://doi.org/10.1038/s41598-022-18511-2

Selek B, Aksu H (2020) Water resources potential of Turkey. In: Water resources of Turkey. pp 241–256. https://doi.org/10.1007/978-3-030-11729-0_8

Selek B, Tuncok IK, Selek Z (2018) Changes in climate zones across Turkey. J Water Clim Change 9(1):178–195. https://doi.org/10.2166/wcc.2017.121

Şen Z (2009) Drought, disasters, and modern computational methods. Water Foundation, İstanbul. (**in Turkish**)

Serkendiz H, Tatli H, Kılıç A et al (2024) Analysis of drought intensity, frequency and trends using the SPEI in Turkey. Theor Appl Climatol 155:2997–3012. https://doi.org/10.1007/s00704-023-04772-y

Simsek O, Ceyhunlu AI, Ceribasi G, Keskiner AD (2024) Evaluation of long-term meteorological drought in the Aras and Çoruh basins with crossing empirical trend analysis. Phys Chem Earth 135:103611. https://doi.org/10.1016/j.pce.2024.103611

Sırdaş S (2002) Meteorological drought modelling and application to Turkey. PhD. Thesis, İTÜ Science Engineering and Technology Institute, İstanbul

Stagge JH, Tallaksen LM, Gudmundsso L, Van Loon AF, Stahl K (2015) Candidate distributions for climatological drought indices (SPI and SPEI). Int J Climatol 35:4027–4040. https://doi.org/10.1002/joc.4267

Thom HCS (1958) A note on the gamma distribution. Mon Weather Rev 86:117–122. https://doi.org/10.1175/1520-0493(1958)086%3C0117:ANOTGD%3E2.0.CO;2

Thom HCS (1966) Some methods of climatological analysis. WMO Technical Note No: 81. Geneva

Thornthwaite CW (1948) An approach toward a rational classification of climate. Geogr Rev 38. https://doi.org/10.2307/210739

Tirivarombo S, Osupile D, Eliasson P (2018) Drought monitoring and analysis: standardised precipitation evapotranspiration index (SPEI) and standardised precipitation index (SPI). Phys Chem Earth 106:1–10. https://doi.org/10.1016/j.pce.2018.07.001

Tuğrul T, Hınıs MA, Oruç S (2025) Comparison of LSTM and SVM methods through wavelet decomposition in drought forecasting. Earth Sci Inf 18:139. https://doi.org/10.1007/s12145-024-01541-x

Turkish State Meteorological Service (2016) Areal precipitation assessment for the year 2015, March 2016, Ankara. (**in Turkish**)

Turkish State Meteorological Service (2025) Maps of PNI - percent of normal index. https://www.mgm.gov.tr/veridegerlendirme/kuraklik-analizi.aspx?d=aylik&k=pni#sfB
Ulupinar Y, Kervankiran S, Akbas AI, Ugurlu A (2015) Areal precipitation assessment of Turkey. In: Proceedings of the VIII. National Hydrology Congress, Sanliurfa, Turkey
Vicente-Serrano SM, Beguería S, L´opez-Moreno JI (2010) A multi-scalar drought index sensitive to global warming: the standardized precipitation evapotranspiration index. J Clim 23:1696–1718. https://doi.org/10.1175/2009jcli2909.1
Wang J, Wang Q, Zhao Y, Li H, Zhai J, Shang Y (2015) Temporal and Spatial characteristics of Pan evaporation trends and their attribution to meteorological drivers in the Three-River source Region, China. J Geophys Res 120(3):6391–6408. https://doi.org/10.1002/2014JD022874
Wang H, Chen Y, Pan Y, Chen Z, Ren Z (2019) Assessment of candidate distributions for SPI/SPEI and sensitivity of drought to Climatic variables in China. Int J Climatol 39:4392–4412. https://doi.org/10.1002/joc.6081
Willeke G, Hosking JRM, Wallis JR, Guttman NB (1994) The National Drought Atlas. Institute for Water Resources Report 94–NDS–4, U.S. Army Corps of Engineers, Washington, DC
Yaman Öz F, Özelkan E, Tatlı H (2024) Comparative analysis of SPI, SPEI, and RDI indices for assessing spatio–temporal variation of drought in Türkiye. Earth Sci Inf 17:4473–4505. https://doi.org/10.1007/s12145-024-01401-8
Yiğit FS, Keten A (2024) General assessment of Türkiye's wetlands. Düzce Univ J Forestry 20(1):348–360. https://doi.org/10.58816/duzceod.1404950
Yıldız D, Özgüler H (2021) According to MGM data, Türkiye is heading toward drought. SPD Hydropolitics Academy, May 10, 2021. (**in Turkish**)
Yılmaz E, Gül MA, Akçay S, Kınacı M (2023) Investigation of the best-fit probability distribution model for SPI-based drought monitoring: a case study from Turkey. Adv Meteorol Article ID 5142965:1–13. https://doi.org/10.1155/2023/5142965
Yu YS, Zou S, Whittemore D (1993) Non-parametric trend analysis of water quality data of rivers in Kansas. J Hydrol 150(1):61–80. https://doi.org/10.1016/0022-1694(93)90156-4
Zarei AR, Shabani A, Moghimi MM (2021) Accuracy assessment of the SPEI, RDI and SPI drought indices in regions of Iran with different climate conditions. Pure Appl Geophys 178:1387–1403. https://doi.org/10.1007/s00024-021-02704-3
Zhang R, Chen ZY, Xu LJ, Ou CQ (2019) Meteorological drought forecasting based on a statistical model with machine learning techniques in Shaanxi Province. China Sci Total Environ 665:338–346. https://doi.org/10.1016/j.scitotenv.2019.01.431
Zhao JC, Wang Z (2020) Future trends of water resources and influences on agriculture in China. PLoS ONE 15(4):e0231671. https://doi.org/10.1371/journal.pone.0231671
Zhao H, Gao G, An W, Zou X, Li H, Hou M (2017) Timescale differences between SC-PDSI and SPEI for drought monitoring in China. Phys Chem Earth 102:48–58. https://doi.org/10.1016/j.pce.2015.10.022
Zhao J, Liu Q, Lu H, Wang Z, Zhang K, Wang P (2021a) Future droughts in China using the standardized precipitation evapotranspiration index (SPEI) under multi-spatial scales. Nat Hazards 109:615–636. https://doi.org/10.1007/s11069-021-04851-1
Zhao X, Xia H, Pan L, Song H, Niu W, Wang R, Li R, Bian X, Guo Y, Qin Y (2021b) Drought monitoring over yellow river basin from 2003–2019 using reconstructed MODIS land surface temperature in Google Earth engine. Remote Sens 13(18):3748. https://doi.org/10.3390/rs13183748

**Publisher's note** Springer Nature remains neutral with regard to jurisdictional claims in published maps and institutional affiliations.

## Authors and Affiliations

**Bülent Selek[1] · Murat Pinarlik[2] · Ismail Faki[3] · Zeliha Selek[2]**

✉ Murat Pinarlik
muratpinarlik@gazi.edu.tr

Bülent Selek
bulentselek53@gmail.com

Ismail Faki
ismail.faki@gazi.edu.tr

Zeliha Selek
zelihaselek@gazi.edu.tr

[1] Ministry of Agriculture and Forestry, Ankara, Turkey

[2] Civil Engineering Department, Faculty of Technology, Gazi University, Ankara, Turkey

[3] Graduate School of Natural and Applied Sciences, Gazi University, Ankara, Turkey